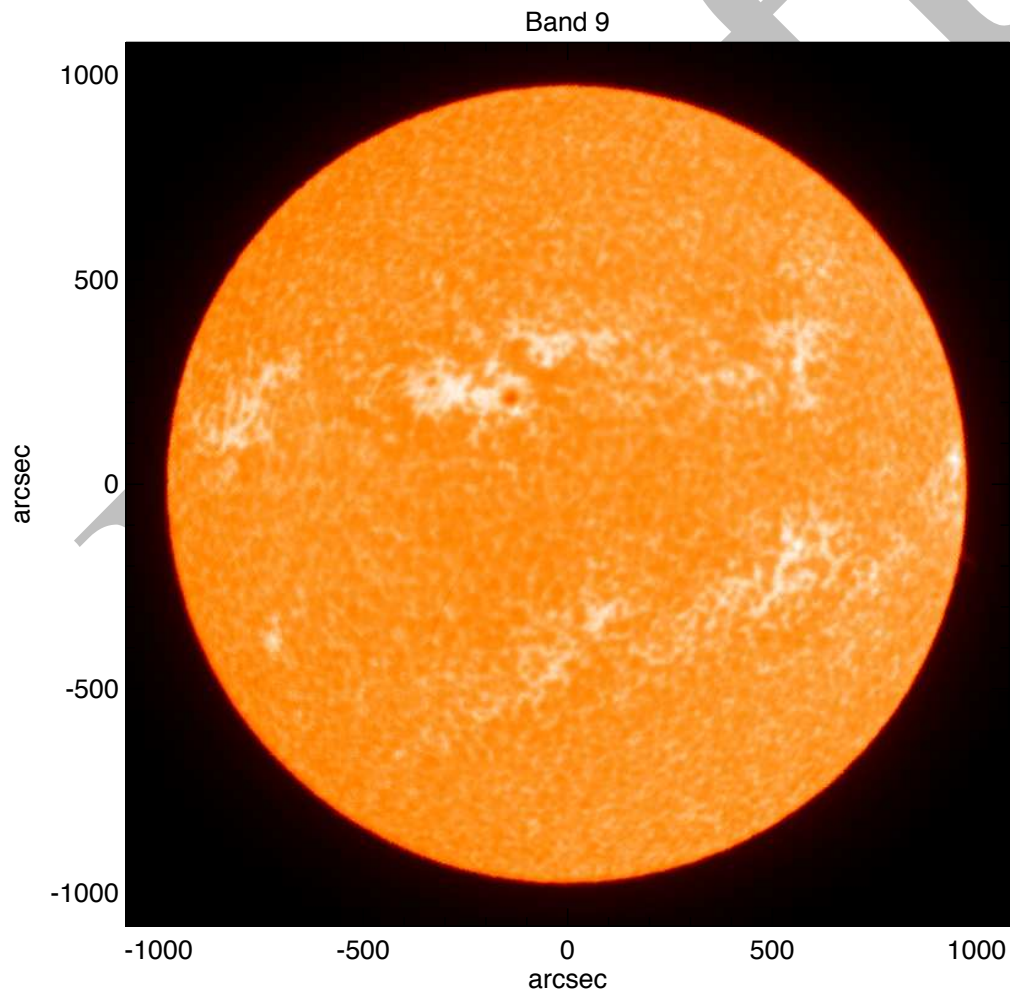


# **Close-out Report:**

## **ALMA Development Study on**

### **Advanced Solar Observing Techniques**

T. S. Bastian (NRAO) and the Solar Development Team



|          |  |           |
|----------|--|-----------|
| <b>1</b> | <b>INTRODUCTION</b>                        | <b>4</b>  |
| <b>2</b> | <b>SOLAR OBSERVING MODES</b>               | <b>5</b>  |
| 2.1      | Solar Filters                              | 5         |
| 2.2      | Mixer De-tuning                            | 6         |
| 2.3      | Additional Considerations                  | 8         |
| 2.3.1    | Water Vapor Radiometers                    | 8         |
| 2.3.2    | IF Attenuator Settings                     | 9         |
| 2.3.3    | Frequency Selection                        | 9         |
| <b>3</b> | <b>MD MODE OBSERVING</b>                   | <b>10</b> |
| 3.1      | Solar Interferometry                       | 10        |
| 3.1.1    | Validation of Interferometric Observations | 10        |
| 3.1.2    | Phase Calibration Transfer                 | 12        |
| 3.1.3    | Bandpass Calibration                       | 14        |
| 3.1.4    | Amplitude Calibration                      | 14        |
| 3.2      | Single Dish Mapping                        | 16        |
| 3.2.1    | Single Dish Mapping: Fast Scanning         | 17        |
| 3.2.1    | Linearity of the MD Modes                  | 19        |
| 3.2.3    | Single Dish Flux Calibration               | 20        |
| <b>4</b> | <b>SINGLE DISH MAPPING OF THE SUN</b>      | <b>21</b> |
| 4.1      | Fast Scanning                              | 21        |
| 4.2      | Full Disk Calibration and Imaging          | 21        |
| 4.3      | Mapping Sub-Regions                        | 25        |
| <b>5</b> | <b>SOLAR INTERFEROMETRY WITH ALMA</b>      | <b>26</b> |
| 5.1      | Calibration                                | 26        |
| 5.2      | Mapping                                    | 28        |
| 5.2.1    | Single Pointings                           | 30        |
| 5.2.2    | Pseudo-mosaic example                      | 34        |
| 5.2.3    | Mosaicking                                 | 35        |
| <b>6</b> | <b>SOLAR OBSERVING: SCIENCE OPERATIONS</b> | <b>35</b> |
| 6.1      | Scheduling Constraints                     | 35        |
| 6.1.1    | Array Configurations                       | 35        |
| 6.1.2    | Shadowing                                  | 35        |

|       |   |    |
|-------|---|----|
| 6.1.3 | Antenna Tracking                                  | 35 |
| 6.2   | Hybrid Antenna Configuration: 7m + 12m            | 36 |
| 6.3   | Calibrator Selection                              | 36 |
| 6.4   | Correlator Mode and Default Observing Frequencies | 36 |
| 6.5   | Solar Scheduling Block                            | 36 |
| 6.6   | Single-dish observing                             | 38 |
| 7     | 2015 SOLAR OBSERVING CAMPAIGN                     | 39 |
| 8     | OUTREACH ACTIVITIES                               | 39 |
| 8.1   | Meetings and Workshops                            | 39 |
| 8.2   | Proceeding Publications                           | 40 |
| 8.3   | Science Review                                    | 41 |
| 8.4   | ALMA Science Simulations Group: SSALMON           | 41 |
| 8.5   | Synergies   | 41 |
| 9     | CONCLUDING REMARKS                                | 42 |

# 1 Introduction

Solar observing was part of the original science case for ALMA but it has not been developed and implemented as a supported observing mode to date. Following the first ALMA Solar Workshop in Glasgow in January 2013, an international team was assembled and proposals were submitted for ALMA Development Studies to the NAASC and to ESO. These were funded in 2014 and the team moved forward with activities necessary to develop, test, and implement solar observing with ALMA with the intention of making solar observing available to the community for the first time in Cycle 4. This goal was successfully met.

Solar observing will be supported as a nonstandard observing mode in as follows:

- Band 3 and band 6 continuum observations of the Sun will be supported
- Solar observing will only be offered for the most compact array configurations
- Both 7m and 12m antennas will be correlated by the baseline correlator
- Both single pointing and mosaicking (up to 150 pointings) interferometric observations of target sources will be supported
- Observations with the interferometer will be supported by fast-scanning total power (TP) maps of the full disk of the Sun

The scientific requirement for 12m + 7m + TP mapping is that the Sun fills the ALMA field of view with structure on all spatial scales; measurements on the widest possible range of uv spacings are needed instantaneously: addition of single dish data fills in the crucial short-spacing data that the interferometer, even when mosaicking, lacks. The support of solar observing in Cycle 4 was predicated on the assumption that each of the above items was satisfactorily demonstrated, that scheduling block (SB) templates would be available for the execution of Cycle 4 solar observations, and that data reduction and mapping procedures in CASA have been developed and implemented in scripts.

In parallel to these activities, significant community outreach activities occurred as a means of advertising ALMA's solar observing capabilities to the solar and space physics communities and to engage the community in defining the science potential of the instrument. These activities included:

- the organization of a simulations group (the SSALMON group)
- the preparation of a peer-reviewed paper (with 38 authors) highlighting ALMA science – published in 2015 in Space Science Reviews
- numerous presentations at professional meetings (enumerated in an appendix)
- the organization of a community workshop highlighting synergies between ALMA, the NSO DKIST O/IR telescope, the NASA IRIS UV mission, to be held from March 15-18, 2016, in Boulder
- an NRAO Live event with tutorials on proposal submission and preparation for ALMA.

This report summarizes the development work conducted by the team and associated outreach activities to publicize the science opportunity represented by ALMA to the solar community.

## 2 Solar Observing Modes

Solar observations with ALMA are possible because the surface of the antennas is designed to scatter the O/IR radiation to an extent that the subreflector and other elements in the optical path are not damaged or degraded. However, additional measures must be taken to allow useful observations of the Sun to be made. ALMA receivers are designed for a maximum RF signal corresponding to an effective brightness of about 800 K at the receiver input. Since the quiet Sun has a temperature of  $\sim 5000\text{--}7000$  K at ALMA frequencies, the solar signal must be attenuated or the receiver gain must be reduced to ensure that receivers remain linear, or nearly so.

### 2.1 Solar Filters

The initial solution adopted by ALMA was the use of a “solar filter” (SF) that is mounted on the Amplitude Calibration Device (ACD) of each antenna. When placed in the optical path the solar filter is required to attenuate the signal by  $4+2\lambda_{\text{mm}}$  dB with a return loss of -25 dB (-20 dB for  $\nu > 400$  GHz) and a cross polarization induced by the filter of -15 dB, or less. There are several drawbacks to this solution (see Yagoubov 2013a):

- The hot and ambient calibration loads cannot be observed when the SF is in the optical path, making amplitude calibration difficult.
- The SNR on calibrator sources is greatly reduced, not just by the attenuation introduced by the filter, but by the thermal noise that is added to  $T_{\text{sys}}$  by the filter itself
- The SF introduces frequency dependent (complex) gain changes that may be time dependent and must be calibrated
- The SFs introduce significant wave-front errors into the illumination pattern on the antenna, resulting in distortions to the beam shape and increased sidelobes
- The Water Vapor Radiometers (WVRs) are blocked by the ACD for many bands when the SF is inserted into the optical path and phase corrections based on WVR measurements are therefore not possible in these bands

Some of these difficulties have been overcome – e.g., the complex gains of antennas outfitted with SFs were measured during the 3<sup>rd</sup> solar observing campaign in 2013 (documented in JIRA ticket CSV-2925) – and interferometric imaging with solar filters has been demonstrated (CSV-2933). In fact, the SFs may be used for observations of solar flares modest size at some future time. Nevertheless, the disadvantages to the use of solar filters are significant. They must be moved out of the beam when observing calibrators, thereby increasing operational overhead. Since they introduce frequency-dependent and possibly time-dependent delays, they must be measured for every filter and frequency setting. Other calibrations – pointing, focus, and beam shape

measurements – need to have the filters in place. The reduced SNR makes such measurements more difficult.

## 2.2 Mixer De-tuning

While the use of solar filters has been demonstrated to work, their use introduces enough disadvantages to consider whether an alternative approach may be more attractive. Yagoubov (2013b, 2014) pointed out that the ALMA SIS mixers could be de-tuned or de-biased to reduce the mixer gain and effectively increase the saturation level to a degree that potentially allows solar observing without the use of the solar filters, at least for non-flaring conditions on the Sun. This idea is illustrated in Fig. 2.1, which shows the SIS current (left axis) and conversion gain (right axis) plotted against the voltage bias for band 5. The normal voltage bias tuning is on the first photon step where the gain conversion is a maximum. However, the mixer still operates at other voltage bias settings. These produce lower conversion gain but since the dynamic range scales roughly inversely with gain, these settings can handle larger signal levels before saturating. In addition to the SIS bias voltage, the local oscillator (LO) power can be altered in order to further modify the receiver performance.

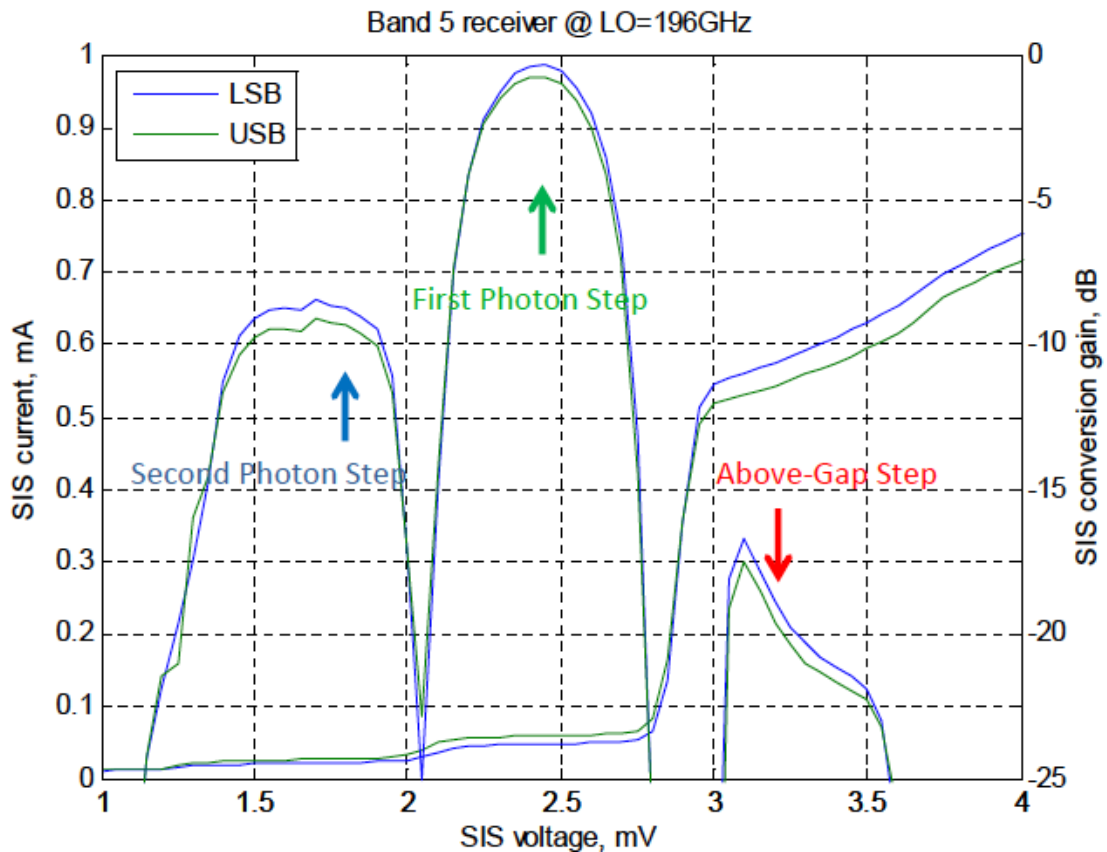


**Figure 2.1** Plot of SIS current and conversion gain as a function of voltage setting.

Lab tests by Yagoubov on band 5 in late-2013 and early-2014 were sufficiently encouraging to perform tests on antennas at the ALMA site. These were executed in April and May of 2014 for additional bands. Typical results for band 3 and band 6 are summarized in tables 2.1 and 2.3, respectively.

Yagoubov concluded that for band 3 the second photon step below the gap has the flattest gain response as a function of SIS bias voltage as well as better linearity and sensitivity than the first step above the gap. He therefore recommended tuning the voltage bias to the second step below the gap for “quiet” Sun observations, referred to as Mixer De-tuning mode 1 (MD1). For “active” Sun observations, he recommended tuning to the second photon step above the gap, referred to as Mixer De-tuning mode 2 (MD2). As mentioned, the LO power can also be adjusted to further optimize performance for solar observations but this has not yet been tested in detail.

**Table 2.1**

| <b>Band 3</b>                                | <b>2<sup>nd</sup> step<br/>below<br/>the gap<br/>(MD1)</b> | <b>1<sup>st</sup> step<br/>below<br/>the gap</b> | <b>1<sup>st</sup> step<br/>above<br/>the gap</b> | <b>2<sup>nd</sup> step<br/>above<br/>the gap<br/>(MD2)</b> |
|--|--|--|--|--|
| <b>Typical Rx noise temperature (K)</b>      | 50   | 40   | 200  | 800  |
| <b>Derived Sky temperature(K)</b>            | 20   | 10-15  | 15-20  | 20   |
| <b>Derived Sun temperature (K)</b>           | ~6000  | ~4500  | 5500-6500  | 6000-6500  |
| <b>Estimated % compression with QS input</b> | 5-10   | 30-35  | 10-15  | 0-5  |

Implementation of band 3 solar observing modes are therefore as follows for an LO frequency of 100 GHz (Table 2.2; see also section 2.3.3):

**Table 2.2**

| <b>Band 3</b>           | <b>LO power</b> | <b>SIS voltage bias</b> |
|-------------------------|-----------------|-------------------------|
| <b>Quiet Sun (MD1)</b>  | Nominal         | 8.5 mV                  |
| <b>Active Sun (MD2)</b> | Nominal         | 13.3 mV                 |

Similarly, for band 6 the test results are summarized in Table 2.3:

**Table 2.3**

| Band 6  | 2 <sup>nd</sup> step below the gap | 1 <sup>st</sup> step below the gap (MD1) | 1 <sup>st</sup> step above the gap (MD2) |
|---|------------------------------------|--|--|
| <b>Typical Receiver noise Temperature (K)</b> | 200                                | 60                                       | 800                                      |
| <b>Derived Sky temperature (K)</b>            | 45                                 | 40                                       | 40-45                                    |
| <b>Derived Sun temperature (K)</b>            | ~4500                              | ~4000-4500                               | ~4500                                    |
| <b>Estimated % compression with QS input</b>  | 0-5                                | 5-10                                     | 0-5                                      |

It was found for band 6 that the second photon step below the gap did not always provide a flat and stable gain response (at least with nominal LO power). Moreover, the receiver gain compression is rather moderate on the quiet Sun even at nominal receiver settings (first step below the gap). Therefore, no change from nominal settings is recommended for “quiet” Sun observing (MD1). For “active” Sun observations, tuning to the first photon step above the gap is recommended (MD2). Implementation of band 6 solar observing modes are therefore as follows for an LO frequency of 239 GHz<sup>1</sup>:

**Table 2.4**

| Band 6                  | LO power | SIS voltage bias |
|-------------------------|----------|------------------|
| <b>Quiet Sun (MD1)</b>  | Nominal  | Nominal          |
| <b>Active Sun (MD2)</b> | Nominal  | 12.5 mV          |

## 2.3 Additional Considerations

The use of MD modes to observe the Sun has obvious advantages, not least of which is that observations of both the Sun and calibrators can proceed in an MD mode without moving the solar filter in and out of the optical path and managing the complexity and overhead associated with calibration when using solar filters. Nevertheless, there are additional considerations when using MD modes.

### 2.3.1 Water Vapor Radiometers

By using MD modes to observe the Sun the ACD is no longer a factor in blocking the WVRs, thereby allowing phase corrections based on WVR measurements to be made for each 12m antenna – at least in principle. When pointing at the Sun, the radiometer signal will be

$$T_{in} = \eta_b T_{sun} e^{-\tau} + \eta_c T_{atm} (1 - e^{-\tau}) + (1 - \eta_c) T_{amb}$$

<sup>1</sup> The band 6 tests were carried out with an LO of 240 GHz. Consideration of spectral lines that



where  $T_{sun}$  is the brightness temperature of the Sun,  $T_{atm}$  and  $T_{amb}$  are the temperatures of the atmosphere and the ambient at the telescope, respectively, and  $\eta_c$  the beam coupling efficiency between the radiometer and the sky and  $\eta_b$  is the fraction of the coupling of the radiometer to the disc of the Sun. We have  $T_{sun} \gg T_{atm}, T_{amb}$  and with  $\eta_b \approx \eta_c$  the first term dominates. The water vapor line is therefore seen in absorption against the Sun in contrast to the usual case where the line is observed in emission. While this is not a problem, the use of the WVRs for solar observing would require changes in the implementation of the WVR correction to the data. This has not been considered in detail because a much more serious problem is that, currently, the WVRs saturate when pointed at the Sun. They are designed to operate over an input range of  $\sim 30$  K (cold sky) to  $\sim 350$  K (internal WVR hot load), with a specification that they should operate up to  $\sim 600$  K. Unless the optical depth of the sky is  $\sim 2.5$  or more, which would represent highly non-optimum observing conditions in any case, the WVRs are expected to saturate on the Sun. This was checked in March 2014 (see [link](#)) and the WVRs were indeed found to be in strong saturation on the Sun. Unless the WVRs are modified or replaced to increase their dynamic range to accommodate the Sun, phase corrections based on WVR measurements will not generally be possible when pointed at the Sun.

For the time being, then, the WVRs cannot be used to correct solar data for phase variations introduced by water vapor along each antennas line of sight, regardless of whether the solar filters or the MD modes are used. As a consequence, solar observations will be largely confined to the use of compact antenna configurations (see §6.1.1).

### 2.3.2 IF Attenuator Settings

Another consideration – again regardless of whether we use solar filters or the MD modes – is the system IF attenuator settings. The input power changes significantly as the antennas move from the (solar) source to a calibrator and back. The IF chain has two variable attenuators (in steps of 0.5 dB) to ensure that signal levels remain within nominal limits: one in the IF Switch and one in the IF Processor. A concern is whether the variable attenuators themselves introduce unacceptable (differential) phase variation between source and calibrator settings, thereby corrupting phase calibration referenced against suitable sidereal calibrators; and whether there are differences between the spectral window bandpass response between source and calibrator scans as a result of attenuator settings. We return to this issue in §3.1.2 when we discuss phase calibration transfer.

### 2.3.3 Frequency Selection

We decided relatively early in the development process to define default LO frequencies within the ALMA frequency bands for testing continuum MD modes and which, ultimately, would be used for early ALMA solar observing (Cycle 4). The rationale was to ensure that the same frequency setups were used for the various tests conducted with an eye toward continuing development in other bands. We included the potential for spectral line observations in selecting the default bands. The memo by R. Hills outlining the default LO frequency selection is available at JIRA CSV-3162 and is summarized in Table 2.5 below.

Table 2.5

| ALMA Band | 3   | 4   | 5   | 6   | 7   | 8   | 9   | 10  |
|-----------|-----|-----|-----|-----|-----|-----|-----|-----|
| LO Freq   | 100 | 152 | 194 | 239 | 336 | 416 | 669 | 861 |

### 3 MD Mode Observing

The Sun is an extremely large source compared to the primary beam of either the 7m or 12m antennas. The primary beam is filled with complex emission when pointing at the Sun, as are the beam sidelobes. The interferometer ultimately measures the brightness temperature contrast relative to the background Sun. As noted earlier, in order to recover the absolute brightness temperature of solar targets, it is necessary to include not only interferometric observations (by the 7m and 12m antennas), but also total power measurements made by a PM antenna. In this section we summarize activities related to testing MD mode observing for both interferometric and single dish total power mapping observations of the Sun.

#### 3.1 Solar Interferometry

Considerable time was spent characterizing the system on calibrator sources in MD modes and testing possible calibration strategies that we summarize here. Details may be found at the JIRA tickets referenced. The tests were executed during EOC time in Jul-Nov 2014, and during the 4<sup>th</sup> Solar Observing Campaign from December 8-15. The tests were typically executed using the script `SunDelayCal_md.py`, a modified version of `SunDelayCal-atm.py`, which was developed for earlier solar campaigns that made use of the solar filters.

##### 3.1.1 Validation of Interferometric Observations

Before investing substantial time in testing MD modes for solar observing, we validated interferometric observing under controlled conditions through computation of closure quantities. These were performed in September 2014 under JIRA ticket CSV-3105. A calibrator source was observed with both nominal SIS mixer settings and with MD settings. Phase closure is illustrated in Fig. 3.1. The first three panels show the raw visibility phases on three baselines, formed by three antennas, for a calibrator source (1924-292) observed in band 6. The first, second, and fourth scans were made with nominal SIS mixer settings and the third scan was made with MD2 SIS mixer settings (Table 2.4). The fourth panel shows the closure phase formed by the three antennas which, despite the larger scatter because of the lower gain and enhanced system temperature, is consistent with zero. Similarly, amplitude closure is illustrated in Fig. 3.2, where the raw amplitudes on four baselines are shown along with the amplitude closure in the bottom panel. Again, the scatter is increased, but the closure amplitude is unity. Given the obvious difference in the complex gain of each antenna when switching between nominal and MD mixer settings, it is highly desirable to observe both calibrators and the Sun in a fixed MD mode. Otherwise, the differential gain between the nominal

and MD observing mode would need to be measured and applied every time solar observations were performed, perhaps repeatedly during a solar observation.

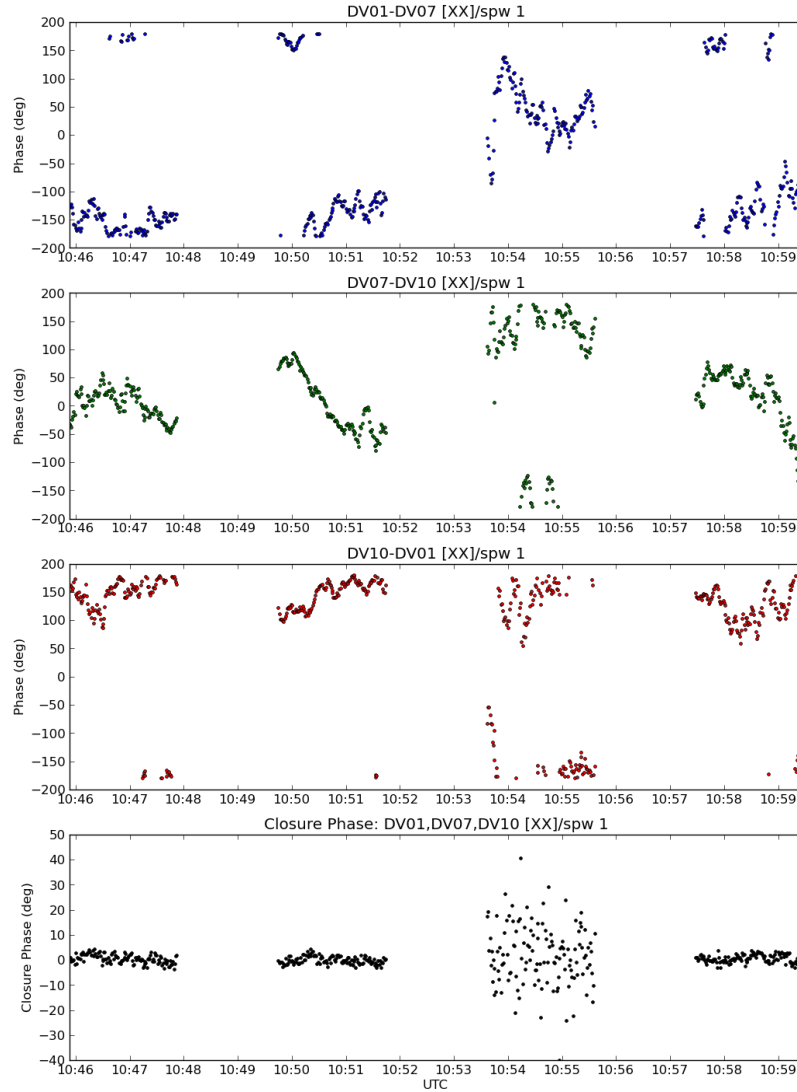


**Figure 3.1:** The top four panels show the visibility phase between DV01-DV07, DV07-DV10, and DV10-DV01, respectively. Phase closure between DV01, DV07, and DV10 is shown in the bottom panel using data obtained in band 6 using both nominal receiver settings (scans 1, 2, and 4) and MD2 receiver settings (scan 3). (Data: uid://A002/X8b8415/Xd4f)

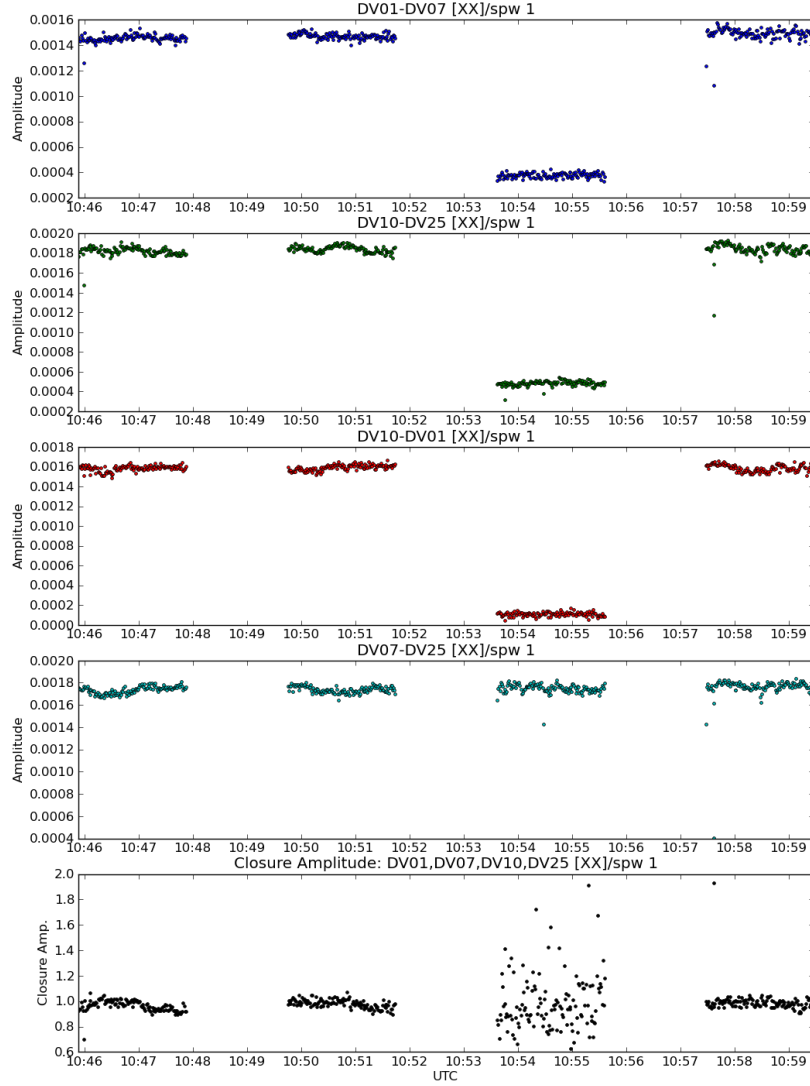


**Figure 3.2:** The top three panels show the visibility amplitude between DV01-DV07, DV10-DV25, DV10-DV01, and DV07-DV25, respectively. Amplitude closure between DV01, DV07, DV10, and DV25 is shown in the bottom panel using data obtained in band 6 using both nominal receiver settings (scans 1, 2, and 4) and MD2 receiver settings (scan 3). (Data: uid://A002/X8b8415/Xd4f)

### 3.1.2 Phase Calibration Transfer

As mentioned in §2.3.2, variable attenuators are used to optimize signal levels in the IF/LO chain. However, when the attenuation levels of the attenuators in the IF switch and IF processor are optimized for the Sun, they are non-optimum for calibrator sources. It is necessary to reduce the attenuation levels relative to the solar values when observing phase and flux calibrators.

The variation in system temperature caused by the stepped attenuators is negligibly small, so we do not need to correct for their influence on flux calibration. On the other hand, the

attenuators do introduce phase shifts (Fig. 3.3), depending on the difference in attenuation introduced for solar and calibrator scans. If the values of the phase shifts in all antennas are identical, the phase shift will be differenced out and the transfer of phase calibration from a calibrator to the solar source can proceed without the added complexity of measuring and applying differential phase corrections to account for phase errors introduced by the IF Switch and IF Processor attenuators.

To evaluate whether the attenuators introduced unacceptable differential phase errors or not, we observed bright quasars while changing the attenuation levels in both the IF Switch and/or IF Processor attenuators in an extensive series of tests during the December 2014 solar observing campaign. These are documented in JIRA tickets CSV-3162 and CSV-3165. Tests were performed using nominal MD1 and MD2 settings for both band 3 and band 6. These tests demonstrated that the differential phases introduced by changes to attenuator settings were generally small, at least on short baselines. The situation was less clear on longer baselines, in part because the time between ATT state changes was rather long (220 s) and the long baselines are more susceptible to changes in the atmosphere.

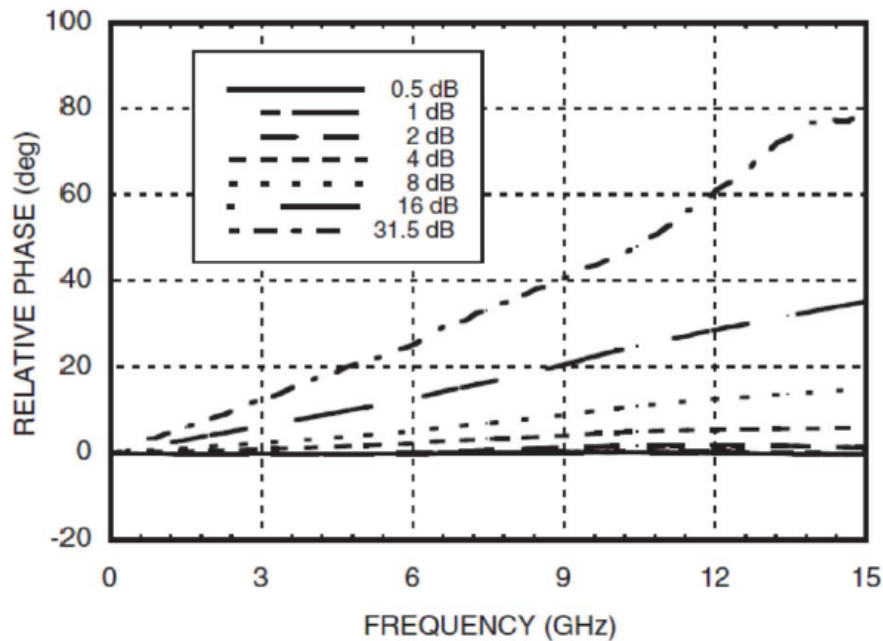


**Figure 3.3:** Phase change introduced by attenuator states ranging from 0.5-31.5 dB.

We therefore repeated the tests in August 2015 using more rapid mode switching (60 s). Fig. 3.4 shows an example from this suite of tests. The other cases (Band 3/6, IFswitch/IFprocessor) show similar results: the residual is typically small, less than  $\pm 1$  degree (maximum:  $\pm 3$  degrees) and the variation of the normalized amplitude is about 1%, in all basebands.

On the basis of these tests we conclude that we do not need to perform additional calibrations to correct for the small differential effects caused by the difference in

attenuator states between source and calibrator scans. The stepped attenuator values adopted for calibrator sources relative to solar values in bands 3 and 6 using modes MD1 or MD2 are summarized in Table 3.1.

**Table 3.1**

| Receiver | MD mode | Difference in Attenuator Levels for Calibrators |             |
|----------|---------|---|-------------|
|          |         | IFswitch  | IFprocessor |
| Band3    | MD1     | -5 dB   | -10 dB      |
|          | MD2     | -7 dB   | 0 dB        |
| Band6    | MD1     | -5 dB   | -10 dB      |
|          | MD2     | -8 dB   | 0 dB        |

While these tests show that phase shifts caused by the attenuation level changes do in practice difference out, verification that this is the case cannot be checked from observing data obtained using the solar scheduling block (SB; see §4.5). As a check, we recommend that a test observation of a calibrator source be executed using normal and MD attenuation levels before solar observations begin on a given day or at least once before a campaign program.

### **3.1.3 Bandpass Calibration**

Bandpass calibration is carried out in the usual manner using MD modes: i.e., a strong calibrator is observed in an MD mode and the bandpass solution is obtained. Bandpass shape and stability were checked for MD modes and attenuator states in bands 3 and 6 as part of our test program during the December 2014 campaign and repeated in August 2015. We found that perturbations to bandpass amplitudes and phases were small. For the IF switch and IF processor settings adopted for MD mode observing (Table 3.1) we find that the rms difference between bandpass phases for an MD attenuator state and the nominal attenuator state was generally a fraction of a degree for both band 3 and band 6, the maximum being 1.2 deg. Similarly, the normalized amplitude difference was typically a fraction of 1%. We conclude that no explicit correction for differential bandpass is needed.

### **3.1.4 Amplitude Calibration**

In the non-solar case, the antenna temperature ( $T_{\text{ant}}$ ) is small compared to the system temperature, and  $T_{\text{ant}}$  can therefore be neglected for amplitude calibration. In contrast, unlike most cosmic sources, the antenna temperature of the Sun is large ( $\sim 7000$  K at 100 GHz). It is therefore necessary to measure both the system temperature and the antenna temperature when pointing at the Sun in order to compute the System Equivalent Flux Density (SEFD) to correctly scale visibility amplitudes.

### Band3 Ifswitch ATT -5dB: Phase Shift & Amp Variation

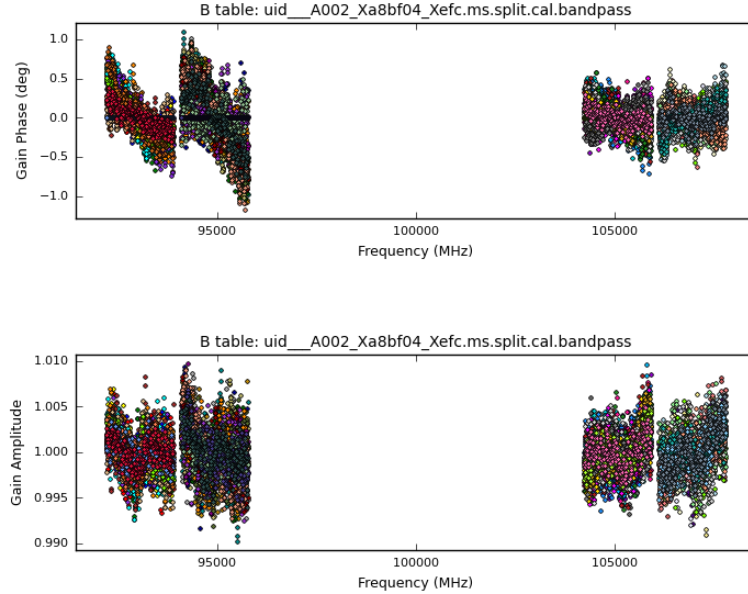


**Figure 3.4:** The residual of the differential phase and the variation of the amplitude for the upper and lower sidebands of band 3. The plot shows the case where the IF Switch attenuator has been reduced by 5 dB; i.e., the setting in the MD mode is -5 dB relative to nominal. (uid://A002/Xa8bf04/Xefc)

To estimate  $T_{\text{ant}}$  on the Sun, “single-dish” measurements must be performed using all antennas of the array. Specifically, the standard observing sequence for solar interferometric observations will include the following measurements:

- a “sky” observation  $P_{\text{sky}}$ , offset from (by typically  $2^\circ$ ) and at the same elevation as, the target (Sun)
- a “cold” load observation  $P_{\text{cold}}$  (also known as the “ambient” load), in which an absorber at the temperature of the thermally-controlled receiver cabin (nominally  $20^\circ\text{C}$ ) fills the beam path;
- a “hot” load observation  $P_{\text{hot}}$ , in which an absorber heated to  $\sim 70^\circ\text{C}$  fills the beam path
- a “zero” level measurement  $P_{\text{zero}}$ , which reports the levels in the detectors when no power is being supplied.

Then the telescope moves to the target (Sun) where the IF attenuation levels are set appropriate to the input power. After the target scan, the telescope again moves to the “sky” position and takes another measurement, called the “off” measurement  $P_{\text{off}}$ , without changing the IF attenuation.

The antenna temperature of the science target is then given by:

$$T_{ant} = (P_{sun} - P_{off}) \frac{(P_{sky} - P_{zero})}{(P_{off} - P_{zero})(P_{hot} - P_{cold})} (T_{hot} - T_{cold})$$

The autocorrelation data output from the baseline correlator cannot be used for this measurement because it has insufficient dynamic range to measure  $P_{zero}$  (Note: the value is sometimes negative). Instead, the necessary measurements rely on total power data obtained by the baseband detectors. Therefore, the observing data of solar interferometric observations must include the total power data obtained by the BB detectors.

Figure 3.5 shows the antenna temperatures derived for all antennas used for a test observation on 1 August 2015 toward active region NOAA 12391. The antenna temperatures obtained for band 3 using MD2 mode are  $\sim 7000$  K, consistent with the value expected at this frequency for an active region. The antenna temperatures obtained with band 3 using MD1 mode in Figure 3.6 is about 6000 K, smaller than that obtained with band 3 using MD2 although the data were obtained on the same day. The MD1 values are the result of mild compression of the receiver response in this mode. We consider the linearity of MD1 and MD2 in more detail in §3.2.2.

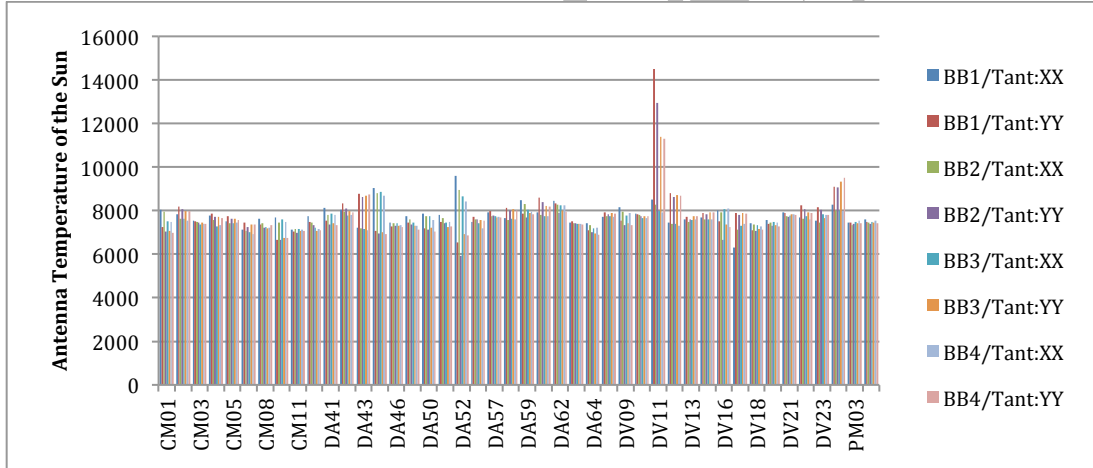


**Figure 3.5:** The antenna temperature of each antenna for band 3 MD2 (uid://A002/Xa72fea/Xd96).

## 3.2 Single Dish Mapping

In this section we summarize tests and strategies relevant to the use of the total power (PM) antennas for mapping the Sun. We anticipate using both interferometry and single dish total power mapping in reconstructing the brightness temperature distribution of solar target.



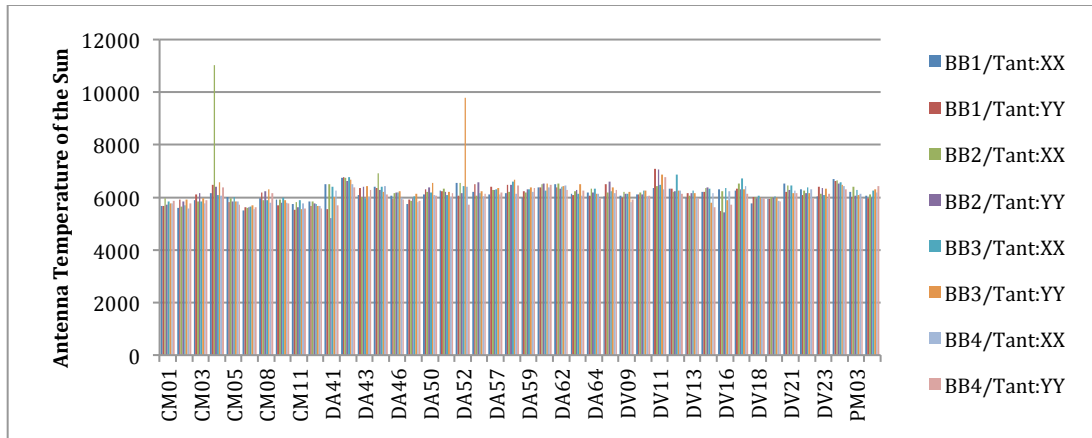


**Figure 3.6:** The antenna temperature of each antenna for band 3 MD1 (uid://A002/Xa72fea/Xfle).

### 3.2.1 Single Dish Mapping: Fast Scanning

Fast-scanning mapping techniques were developed by R. Hills and colleagues, as originally documented under JIRA CSV-239, during the “fast scanning campaign” in September 2014 and, in the solar context, during the December 2014 solar observing campaign as documented under CSV-3166. Fast scanning observations are ideal for recovering the flux or brightness distribution on angular scales ranging from the ALMA primary beam width to the scale of the target in question (typically a few arcminutes), or up to the full disk of the Sun.

Briefly, fast-scanning entails making total power (and more recently, autocorrelation measurements) as the telescope pointing is driven continuously and smoothly through a sampling pattern on the target that avoids sudden acceleration or deceleration of the antenna drive motors. A major advantage of fast scanning is that it minimizes the impact of atmospheric variation, and the full solar disk can be mapped in as little as 6 minutes. However, successful use of fast-scan mapping with the total power PM antennas requires careful characterization of their servos.

Two types of scan patterns have been developed and tested for ALMA dishes: Lissajous patterns, which map a rectangular region of the sky; and a “double circle” patterns, which map a circular region on the sky (Fig. 3.7). These may be used with a great deal of flexibility with respect to the angular area mapped in total power.

Both these patterns have been tested for solar mapping and shown to work well. The double-circle pattern is particularly well suited for full-disk mapping because its coverage matches the shape of the solar disk and it repeatedly revisits the region of the center of the disk, allowing atmospheric opacity variations to be addressed. We expect that we will exclusively use the double-circle pattern in cycle 4, in anticipation that all single-dish mapping will be full-disk. Figure 3.8 shows a Band 6 solar image obtained using the double-circle pattern with antenna PM02 on 2015 April 18: this image shows a striking network pattern in addition to bright active regions and darker cooler regions with some

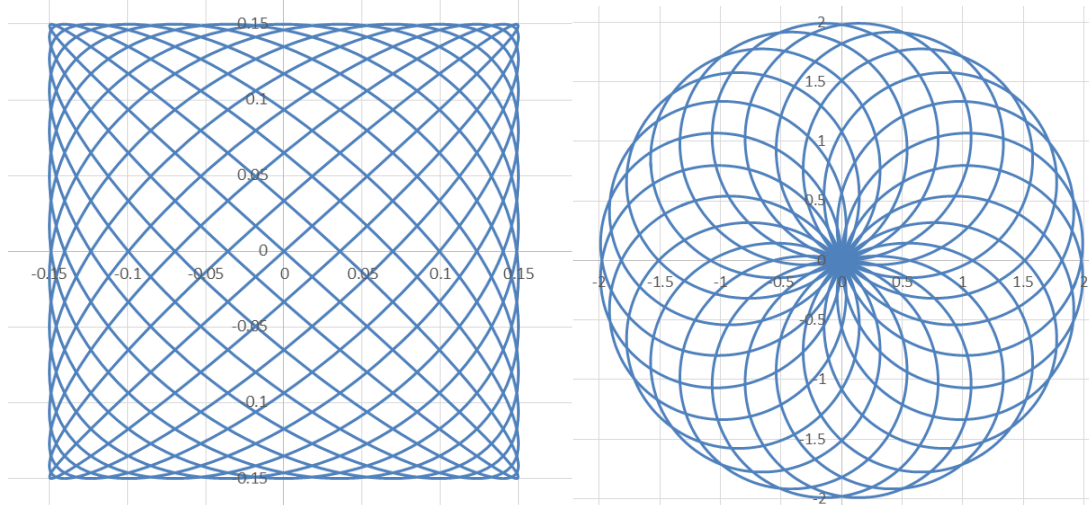


**Figure 3.7:** Examples of Lissajous (left) and double-circle (right) scan patterns used to map the full disk of the Sun or sub-regions of the Sun. Actual patterns sample the source more densely to ensure that it is no less dilute than Nyquist sampling.

limb brightening. The Lissajous pattern would be appropriate for mapping smaller regions of the Sun where the square shape of its field of view is likely to be a better match to images from observatories at other wavelengths.

Commissioning of fast-scan mapping with the ALMA dishes demonstrated that the servos of the dishes have to be adequately characterized. The usual sample rate for total-power measurements is every 2 milliseconds, and the timing associated to each TP measurement has to be shifted (by 0.75 milliseconds and half the sample rate) in order to place the data correctly on the sky. Commissioning work and servo characterization has focused on the PM antennas and we expect that only those antennas will be used for single dish mapping. Standard observing procedures include focus and pointing checks on suitable sources prior to the fast-scan mapping.

### 3.2.1 *Linearity of the MD Modes*

An important issue for calibration is whether the detuned receiver modes place solar observations in a linear regime. We examined the linearity of the receiver system using the Sun itself with single-dish total power observations (JIRA CSV-3171). We observed the Sun using different tuning conditions almost simultaneously. We assumed that the SIS device outputs a lower signal power under conditions for which the gain has been reduced. For example, if we input the same signal, the output level of the MD2 mode should be lower than that of the MD1 mode. Hence, if two output levels derived under different tuning conditions exhibit linearity, this indicates that neither mode is saturated. Figure 3.9 shows the scatter plots obtained for scans across the Sun using the nominal (“normal”) SIS mixer tunings, the MD1 tuning, and the MD2 tuning for bands 3 and 6. The red and green lines show the fitting results obtained using a signal derived inside the disc region and off the solar limb, respectively. The scatter plots are obtained by plotting normal, MD1, and MD2 modes against each other. We conclude from these that the

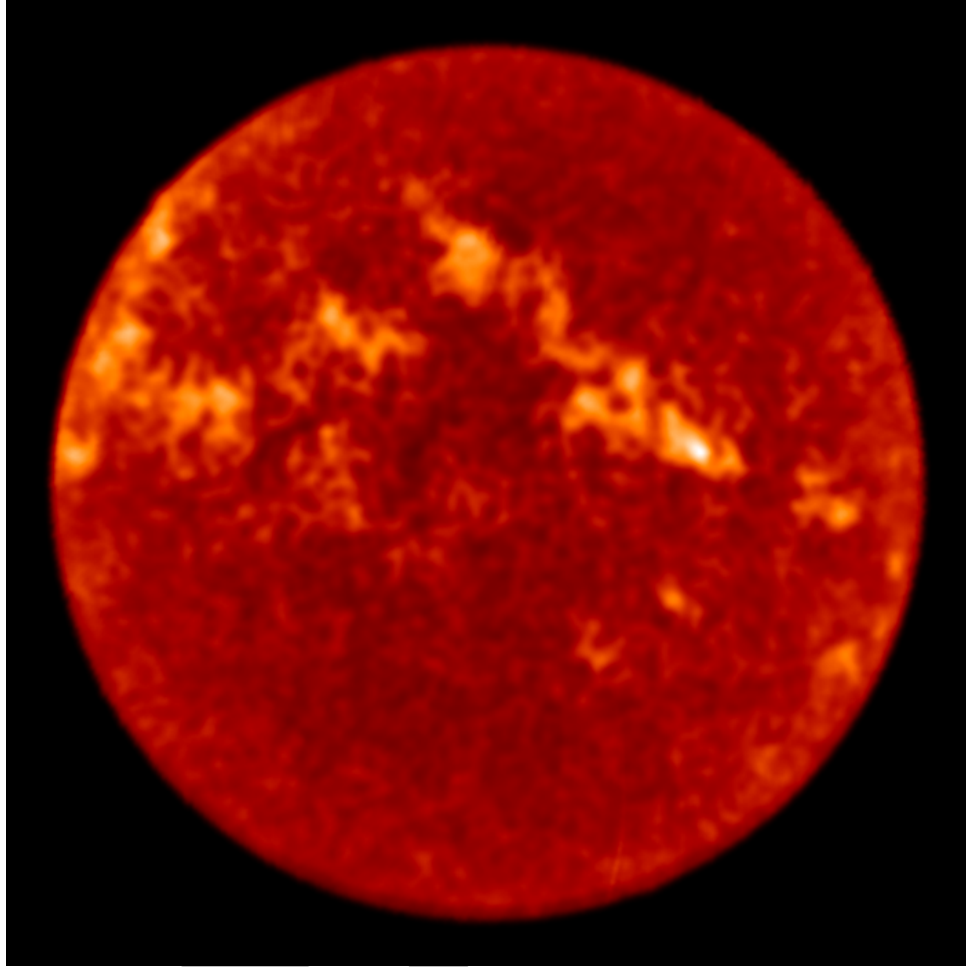


**Figure 3.8:** Full-disk image of the Sun in Band 6 obtained with double-circle fast-scanning on antenna PM02 on 2015 April 18. Structure is seen in this image down to the nominal beam size of 20 arcsec. The contrast represents brightness temperature structure in the solar chromosphere: the network/cell pattern visible across much of the disk is due to convection cells, while active regions are bright and darker filamentary features may be filament channels.

normal, MD1, and MD2 modes are linear for the purposes of calibration and off-limb pointing, but are in saturation when pointing at the solar disk, displaying moderate compression. If we assume that the MD2 mode of Band 3 is not saturated, the MD1 mode underestimates the actual solar level by about 12%. Similar results are obtained for band 6 (13%).

From these results, we recommend using the MD2 mode for single dish observations. Although the MD2 mode is likely not saturated, its linearity should be confirmed by cross-comparison with an MD mode that reduces the gain still further, a test that will be executed in early 2016.

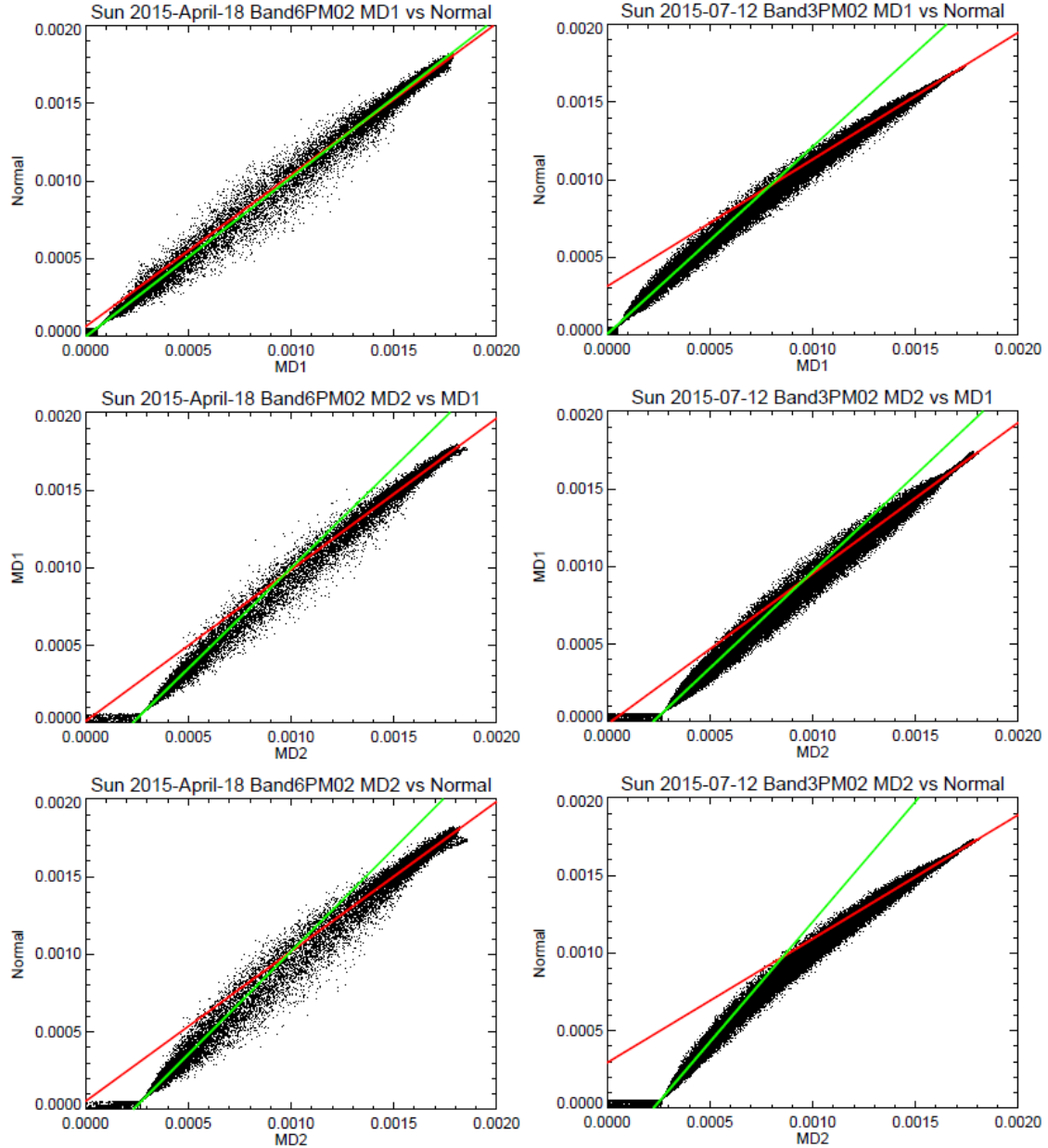


**Figure 3.9:** Scatter plots of solar output levels for two different mixer modes of (left) Band 6 and (right) Band 3: (top) Normal and MD01; (middle) MD01 and MD02; and (bottom) MD02 and Normal. The red and green lines show the fitting results obtained using a signal derived inside the disc region and outside the limb, respectively.

### 3.2.3 Single Dish Flux Calibration

The antenna temperature is determined using the same scheme as that outlined in §3.1.4 as documented by White & Iwai (2015; see CSV-3171). Standard power measurements are obtained on the sky and the hot and ambient loads with normal IF attenuation, on the sky with IF attenuation set for the Sun, and a zero-input-power measurement (the latter is less important when observing with MD2 bias because the increased system temperature in that state makes zero-input-power measurement much smaller than all the other

measured powers). It is straightforward to show (see CSV-3171) that these measurements together with atmospheric opacity are sufficient for amplitude calibration. Since we do not have WVR measurements for atmospheric opacity, we propose to use one of the PM antennas for sky dips at regular intervals in order to track atmospheric opacity during solar observing.

## 4 Single Dish Mapping of the Sun

Solar TP test data were imaged using CASA and IDL. IDL was used as a quick means of mapping fast-scanning TP data and comparing the results with those produced by CASA. The CASA script used for calibration and mapping of solar single-dish data is given in Appendix A.

### 4.1 Fast Scanning

An important goal of the commissioning effort is to ensure a path to calibrated science-quality single-dish fast-scanning images using CASA, and efforts during 2015 have been made jointly with CASA and ALMA team members to identify and then rectify any issues with the CASA analysis path. Recent releases of CASA are reliably able to image fast-scanning maps of the Sun. In order to confirm this, we have been comparing data processed through CASA with an independent calibration and imaging path implemented in IDL. As described in the companion document (ALMA Solar Observing I: Tests and Validation), the imaging aspect of fast-scan data has to take into account some hardware features, notably a timing issue identified by Richard Hills and Neil Phillips, and in addition it relies on utilized antennas having had their servos characterized: if this is not the case, the fast-scan patterns are not executed correctly and we generally see holes in the center of the resulting images.

To demonstrate that the CASA imaging path is now viable, Figure 2.1 compares an image from 2015 April 18 processed with CASA (left panels) with the same data processed through the independent IDL path (right panels; note that the IDL software does not attempt to reproduce the details of the steps such as gridding technique and smoothing that CASA uses for imaging) for two different PM antennas. It is clear from this comparison that CASA is able successfully to image the fast-scanning data.

### 4.2 Full Disk Calibration and Imaging

As described in the companion document, the standard fast-scan solar mapping script (*FastScanObs\_md.py*) makes a number of measurements at the start of each observation for amplitude calibration:  $P_{\text{sky}}$ ,  $P_{\text{hot}}$ , and  $P_{\text{cold}}$  are the power as measured on the blank sky (usually 2 degrees offset from the Sun in azimuth), hot load and ambient load, respectively, with IF attenuation at normal levels;  $P_{\text{zero}}$ , the power measured with no input power from the receiver;

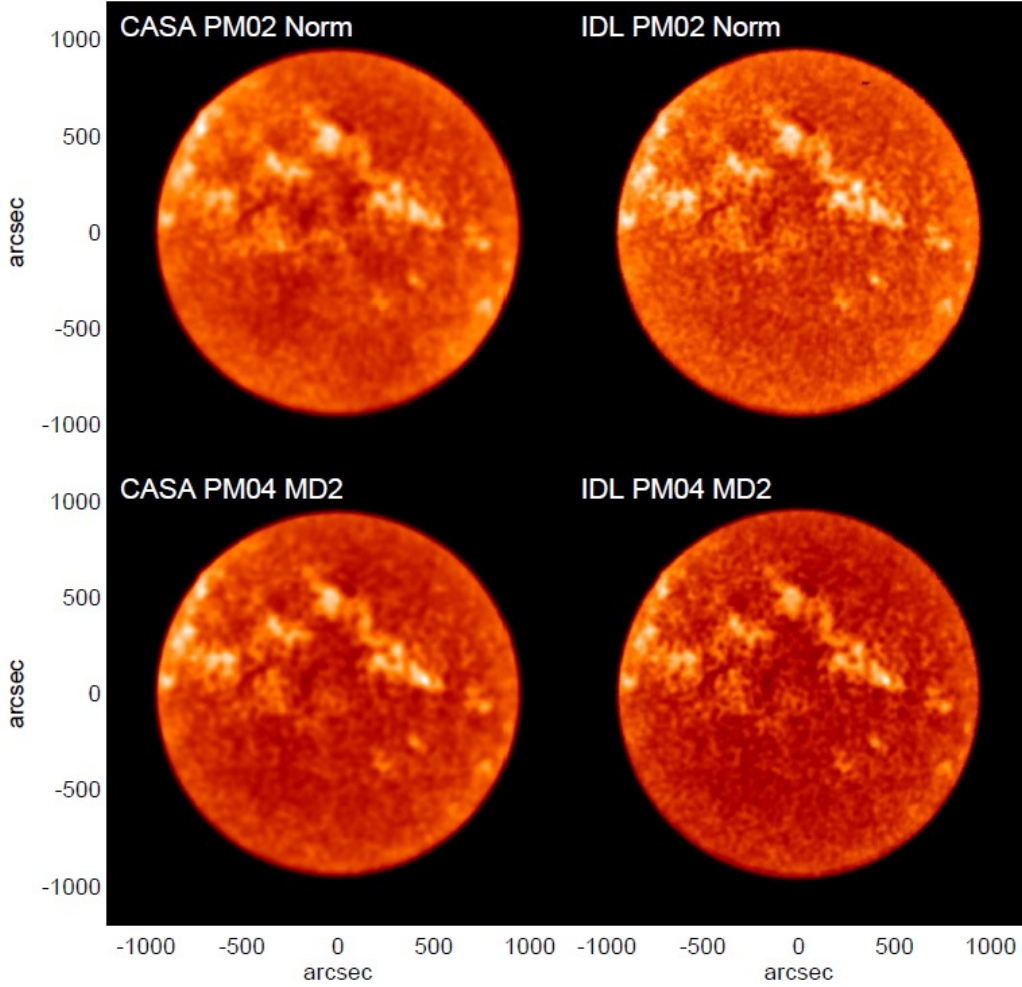


Figure 2.1. Images of the Sun with CASA calibration and imaging (left column) and IDL dual-load calibration and imaging (right column) on Apr 18 for two PM antennas and two bias settings (as labelled). Each image is a single 2 GHz spectral window in band 6 (221 GHz) in XX polarization. Since the data with different bias settings were taken at different times, there are some differences between the upper and lower images due to variable features. The displays are scaled to the square of the brightness temperature to emphasize surface structure. The IDL images have undergone less smoothing than the CASA images.

and  $P_{\text{off}}$ , the power measured on the sky with the IF attenuation set for solar power levels. Then if the atmospheric attenuation  $\tau$  and filled-beam aperture efficiency  $\eta$  are known, power measurements  $P_{\text{src}}$  can be converted to calibrated brightness temperatures via the following expression:

$$T_{\text{src}} = \frac{P_{\text{sky}} - P_{\text{zero}}}{P_{\text{off}} - P_{\text{zero}}} \frac{P_{\text{src}} - P_{\text{off}}}{P_{\text{hot}} - P_{\text{cold}}} \frac{T_{\text{hot}} - T_{\text{cold}}}{\eta e^{-\tau}} + (e^{-\tau} - 1)T_{\text{atm}}$$

where  $T_{\text{hot}}$ ,  $T_{\text{cold}}$  and  $T_{\text{atm}}$  are the temperatures of the hot load, ambient load and the sky layer that contributes most to sky opacity. Derivation of this expression is given in a document



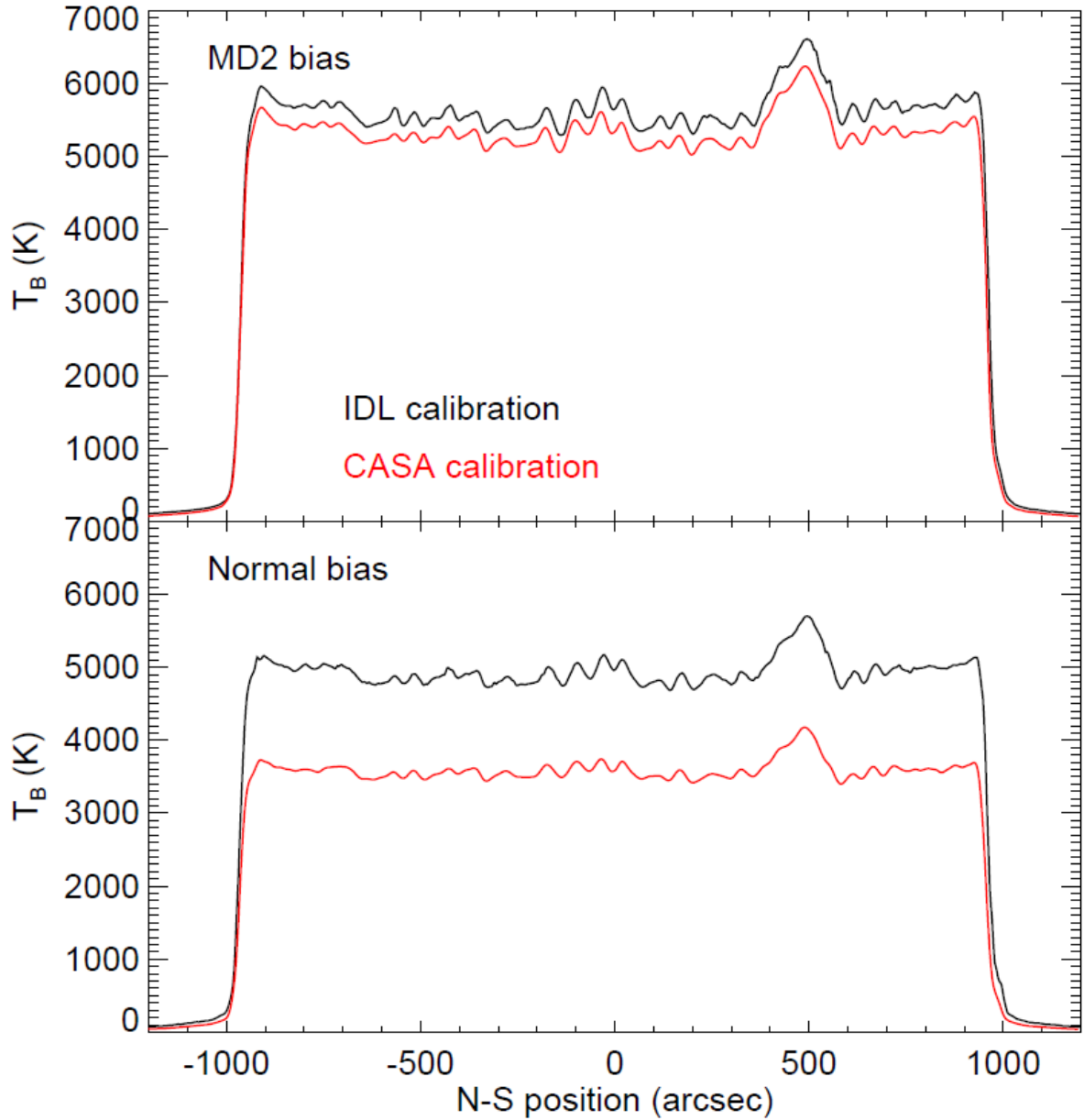


**Figure 2.2:** North-south profiles through the center of the Sun in polarization XX in one sideband (221 GHz) for two receiver bias settings, comparing calibration with the IDL path (black lines) with that applied in CASA (red lines). The upper panel shows the results for the MD2 receiver bias which is planned to be used for solar single dish work; the lower panel shows the results for normal receiver bias, in which the disk temperature in the CASA calibration is much lower.

attached to CSV-3171. This calibration is implemented in the IDL analysis path. Note that it presumably differs from the dual-load calibration method that we assume is used in the CASA analysis. Figures 2.2 and 2.3 compare the results of amplitude calibration through CASA and through the independent IDL path. In Figure 2.2 we show north-south profiles through disk center for both MD2 and normal receiver bias, for the same polarization and frequency.

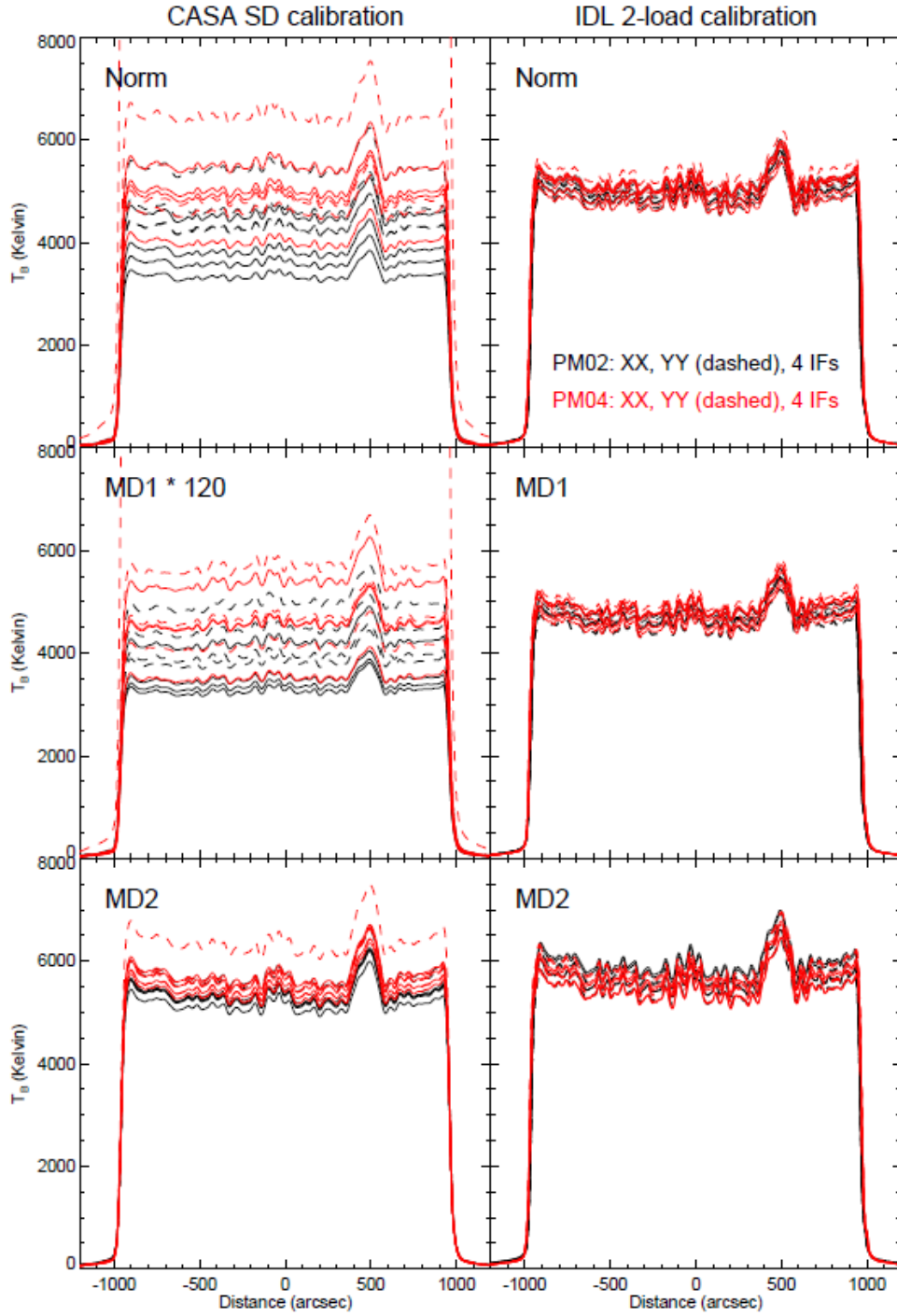


**Figure 2.3:** North-south profiles through the center of the Sun for normal, MD1 or MD2 settings, as labeled) and both CASA calibration (left panels) and IDL calibration (right panels). The curves in each panel for each band are the 4 sidebands in polarizations XX (solid lines) and YY (dashed lines) for both PM02 (black lines) and PM04 (red lines). Note that in the middle left panel the calibrated  $T_B$  values were very low for unknown reasons and they have been multiplied by 120 for presentation on a scale similar to the other panels to show the degree of variation.



The spatial structure is consistent between the two analysis paths in detail, but whereas there is only about a 5% difference between the two calibrations for MD2 bias, the difference is much worse for normal bias. This result is emphasized in Figure 2.3, where we compare the results for all 3 bias settings and plot both XX and YY polarizations for all four 2 GHz-wide continuum frequency bands in band 6, for two PM antennas. The IDL calibration path (note that we do not have an opacity measurement and have to guess at an appropriate value for the analysis) gives consistent amplitude calibration to generally within about 5%, but the CASA calibration with normal and MD1 receiver bias show a much larger range of variation. The CASA calibration for MD2 bias shows 15 of the 16 images to be very close to each other and to the IDL calibration, with one anomalous outlier. Both CASA and IDL calibrations give smaller brightness temperatures for normal and MD1 bias than for MD2 bias. We speculate that this difference results from the fact that the CASA calibration path ignores  $P_{\text{zero}}$ : as shown in the calibration equation above, the scaling to brightness temperature depends on a term  $(P_{\text{off}} - P_{\text{zero}})$  in the denominator.  $P_{\text{zero}}$  is a stable number that varies with antenna, polarization and IF sideband, but is generally very stable in time (over periods of weeks). With normal IF attenuation used when calibrating most cosmic sources,  $P_{\text{sky}}$  (equivalent to  $P_{\text{off}}$  here) is much larger than  $P_{\text{zero}}$  and the subtraction is irrelevant, hence we believe ignored in the normal CASA calibration, but in the case of the Sun  $P_{\text{off}}$  is measured with large IF attenuation and this reduces it to a value that can be close to  $P_{\text{zero}}$ . In the examples shown here, with normal and MD1 receiver bias in band 6  $P_{\text{zero}}$  can be as high as 20-30% of  $P_{\text{off}}$ , which will affect the amplitude scale by the same amount. But in both those cases the system temperature is around 130 K; with MD2 bias the system temperature is around 1100 K and  $P_{\text{zero}}$  is at most 4% of  $P_{\text{off}}$ , so that ignoring  $P_{\text{zero}}$  does not have a marked impact.

In summary, for observations taken with MD2 bias as proposed for solar single-dish work, the CASA calibration is within 5% of the independent IDL calibration and therefore should be suitable for solar data reduction. We believe that the CASA solar SD calibration could be improved by taking  $P_{\text{zero}}$  into account.

### 4.3 Mapping Sub-Regions

During the December 2014 campaign we tested mapping of smaller regions of the solar using fast-scanning Lissajous patterns. Serendipitously, a small flare occurred in the region being mapped, and Figure 2.4 demonstrates the ability of fast-scanning mapping to carry out time-resolved science: these are band 3 images of a region 6 arcminutes on a side, each with a duration of order 30 seconds, clearly showing the compact flare brightening (this observation was made with PM01 with the bad subreflector so that the effective beam size is larger than it should be).

This observation demonstrated that the PM antennas are able to map regions of the solar disk of scientific interest with a cadence of 30 seconds, which is adequate for some flare science and for chromospheric oscillation studies (dominant periods of 180-300 s).

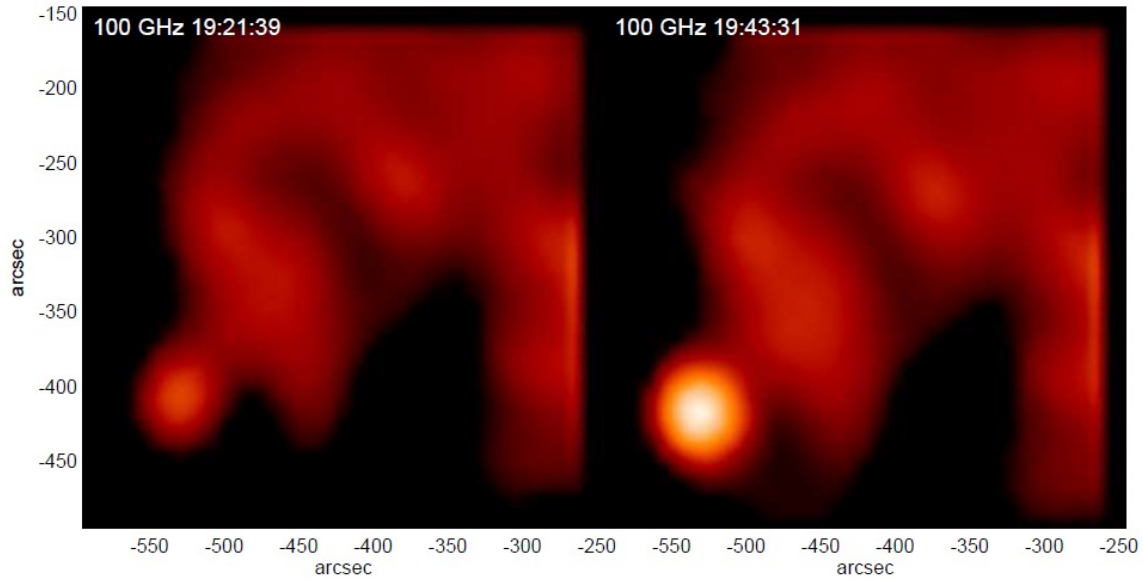


**Figure 2.4:** 100 GHz images of a 6 arcmin  $\times$  6 arcmin region of the solar disk including active region AR 12337 on 2014 December 14. The two images, each required about 30 seconds of mapping using a fast-scanning Lissajous pattern with antenna PM01. A small flare brightening is clearly seen in the compact feature in the lower left of the field of view.

## 5 Solar Interferometry with ALMA

Solar interferometric test data were calibrated and imaged using CASA and AIPS. Recognizing that CASA is the accepted software platform for ALMA data reduction, the emphasis has been on developing scripts that will allow users to successfully imaging continuum data in band 3 and band 6. However, it has been enlightening to crosscheck CASA results using AIPS.

### 5.1 Calibration

As discussed in previous sections there is no mode switching - between the MD mode and normal mode - during the execution of a solar scheduling block. Therefore, the phase variation introduced by use of the MD mode is calibrated by normal phase calibration. Moreover, we need no additional process for dealing the phase variation caused by the attenuator changes because the phase variation of an antenna is similar to each other and they are canceled out. Similarly, the bandpass and flux calibrations for solar data are the same as that for non-solar data (see sections 3.1.2 & 3.1.3).

Special treatment for solar data is needed for the amplitude calibration of visibilities, because the antenna temperature of the Sun cannot be ignored in estimating the System Equivalent Flux Density (SEFD). The measurements for estimating the antenna temperature of the Sun are executed by each scheduling (executing) block. In the CASA calibration script (attached in Appendix B), the antenna temperature of the Sun at each scan is estimated from the values obtained with the baseband (square-law) detector. It means that we can estimate only one antenna temperature in each baseband of each

antenna. Since the emission from the Sun in the observing frequency range of ALMA is continuum basically, the single value for each baseband is enough for the calibration. We note that the “Analysis Utilities” package is necessary to estimate the antenna temperature by CASA because the value of each sub-scan has to be handled.

The amplitude of visibility ( $S_{cij}$ ) and SEFD are written as follows

$$S_{cij} = \rho_{ij} \sqrt{SEFD_i SEFD_j} \quad SEFD = \frac{2k(T_a + T_{sys})}{A_e}$$

where  $\rho_{ij}$  is a normalized cross-correlation coefficient,  $T_a$  is the antenna temperature,  $T_{sys}$  is the system temperature,  $k$  is Boltzman constant,  $A_e$  is the effective antenna corrective area;  $i$  and  $j$  indicate individual antennas. To obtain the amplitude of solar visibility from the normalized cross-correlation coefficients, new calibration table “ $T_a + T_{sys}$ ” is made from the  $T_{sys}$  table and the estimated antenna temperatures (Figure 3.1), and is applied to solar data (Figure 3.2).

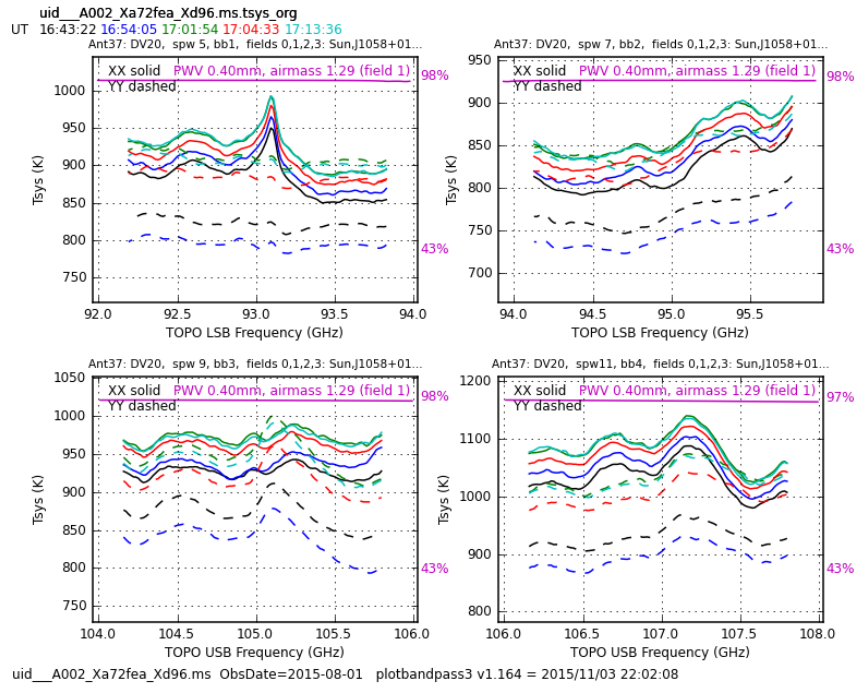


**Figure 3.1:**  $T_{sys}$  of DV20 in band3, MD2, for XX (solid) YY (dashed) polarizations. The different colors indicated different times. (uid://A002/Xa72fea/Xf1e)

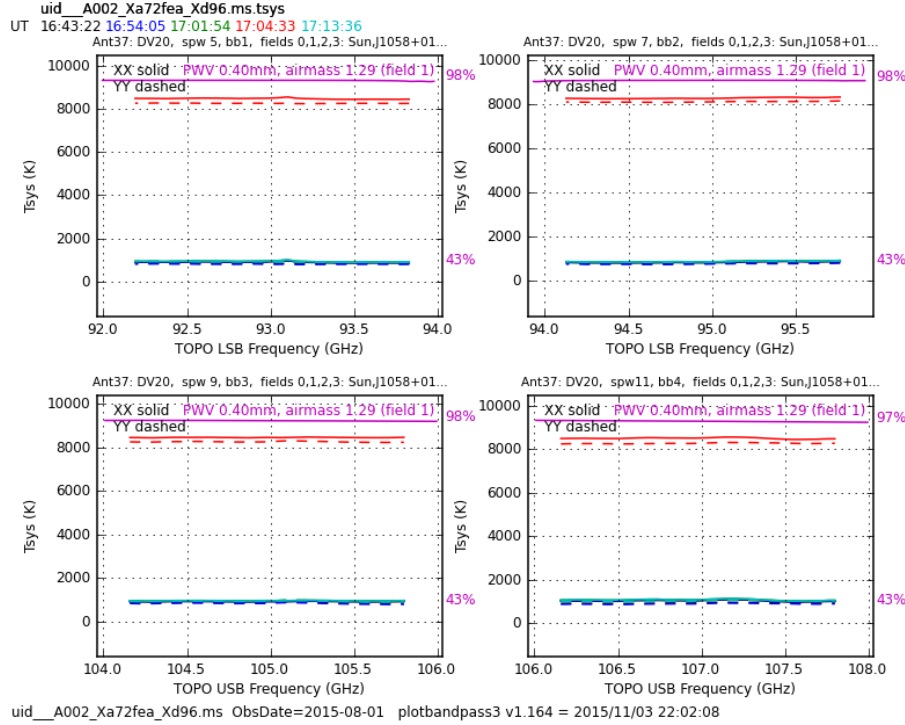


**Figure 3.2:**  $T_a + T_{\text{sys}}$  of DV20 in Band3, MD2, for XX (solid) YY (dashed) polarizations. The different colors indicated different times. (uid://A002/Xa72fea/Xf1e)

The method and process of the amplitude calibration for solar data was established from the data obtained at the test observations in August 2015. Therefore, the amplitude calibration cannot be applied to the solar data obtained at the solar campaign held in December 2014. In section 3.2, we show the solar synthesized images obtained in the campaign. In order to derive an amplitude calibration for these data, we assumed that the antenna temperature of the Sun is 7000 K and there is no dependence on antenna, time, or target region.

## 5.2 Mapping

Since the hybrid antenna configuration (heterogeneous array) comprised of 12m and 7m antennas is used for solar observing, image synthesis must treat the difference in the two primary beams correctly, which the CLEAN task of CASA supports. The options and parameters of the CLEAN task for ALMA solar observing are selected based on the reduction guide of CARMA that is included in the CASA guide<sup>2</sup>.

In most cases, the Sun covers whole the field of view. Therefore, the DC component and angular scales comparable to the field of view are resolved out, and solar synthesized images include imaging artifacts and do not accurately represent the brightness distribution and flux scale of the emission. To obtain the absolute flux of a solar structure it is necessary to combine TP and interferometric data (e.g., through feathering). However, the examples of solar maps included in this section have not done so. They

<sup>2</sup> [https://casaguides.nrao.edu/index.php/CARMA\\_spectral\\_line\\_mosaic\\_M99](https://casaguides.nrao.edu/index.php/CARMA_spectral_line_mosaic_M99)

simply illustrate that it is possible to calibrate and image solar data acquired by the hybrid array. The combination of TP and (mosaicked) hybrid array data will be demonstrated during the December 2015 solar observing campaign.

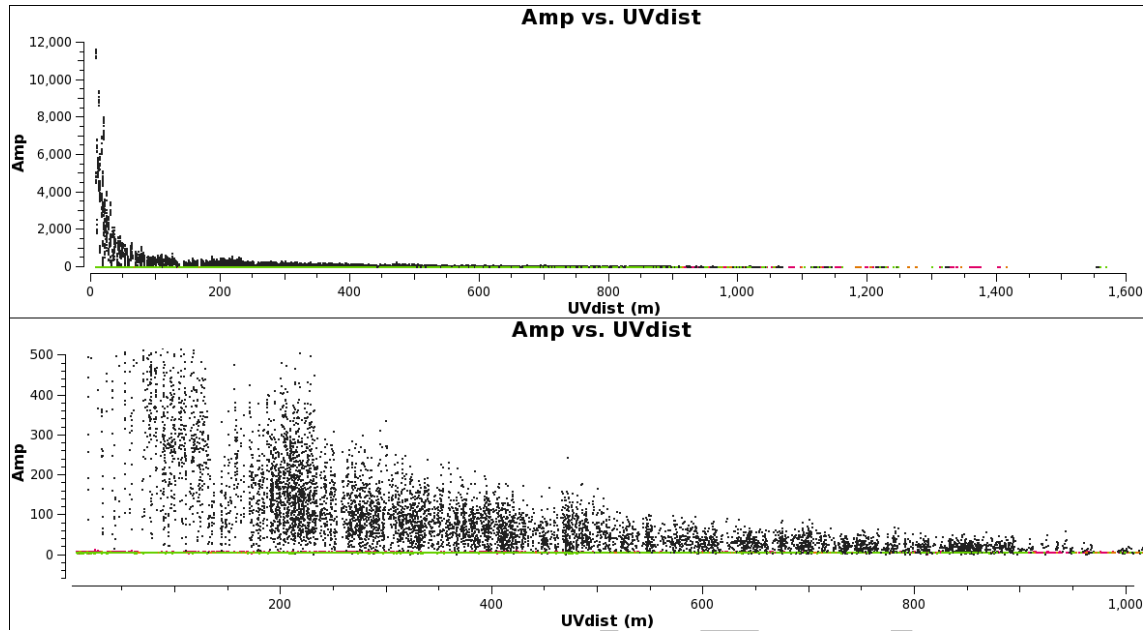


**Figure 3.2:** Calibrated amplitude of visibility as a function of uv-distance. Both panels are made from the same data obtained with Band3-MD2 on 1 August 2015 (uid://A002/Xa72fea/Xfle). Upper panel: Full range of amplitude, Lower panel: Lower range. Black: Target (Sun), colors: Calibrators.

Here, we show examples of synthesized solar images obtained during the solar campaign in December 2014, as well as a test observation from August 2015. We had not developed the amplitude calibration methodology at the time of the December 2014 campaign. Instead, we *assumed* that the antenna temperature was 7000 K for the purpose of converting correlation coefficients to calibrated visibilities. The actual antenna temperatures likely deviated from this value. Test data obtained in August 2015 performed an amplitude calibration as summarized in the companion document.

In all cases, during the deconvolution stage, we used a CLEAN box that included source flux down to the  $\sim 20\%$  level of the combined primary beam. The self-calibration was not performed in the solar image synthesis based on CASA for these tests. The script used for imaging of solar interferometer data is given in Appendix C.

Although the images in next section are made from the data accumulated in 10~30 minutes, similar images result from a snapshot (1 sec).

### 5.2.1 Single Pointings

Example 1: Active region NOAA12230 observed on 14 December 2014

- JIRA ticket: CSV-3167
- Data ID: uid://A002/X96b03d/X2d8
- Receiver: Band3
- MD mode: MD2

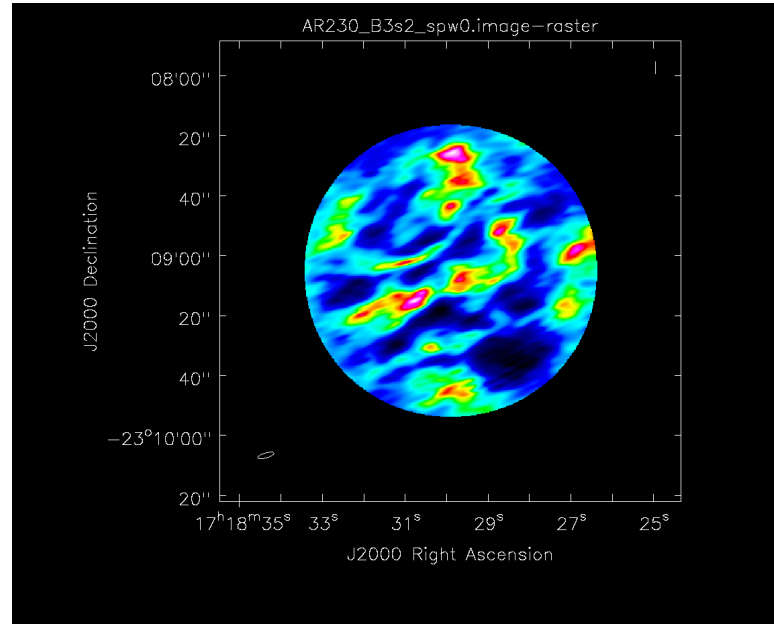


**Figure 3.3:** NOAA12230 observed with Band3-MD2 Synthesized by CASA

This target was also calibrated and imaged in AIPS, which confirmed the basic source structure filling the primary beam.

Example 2: NOAA 12391 observed on 1 August 2015

- JIRA ticket: CSV-3204
- Data ID: uid://A002/Xa72fea/Xd96
- Receiver: Band3
- MD mode: MD2

This observation was carried out using the scheduling block that includes the measurements for estimating the antenna temperature, so the amplitude of visibility is calibrated correctly. On the other hand, the antenna configuration of the 12-m array at the time of the observation was not suitable for solar imaging: the C34-5 configuration is too extended and the solar brightness distribution is therefore significantly under-sampled on short baselines, with the 7m antennas dominating. The ALMA image shown in Figure 3.4 is the DIRT map. Nevertheless, the brightness distribution region in the ALMA image roughly corresponds with the outline of solar plages seen in a 1700 Å chromospheric



image obtained with the Solar Dynamics Observatory AIA telescope. The attached calibration and imaging scripts in Appendices A and B were developed based on the data. The calibration script is similar to that for using in QA2 process by the ARCs.

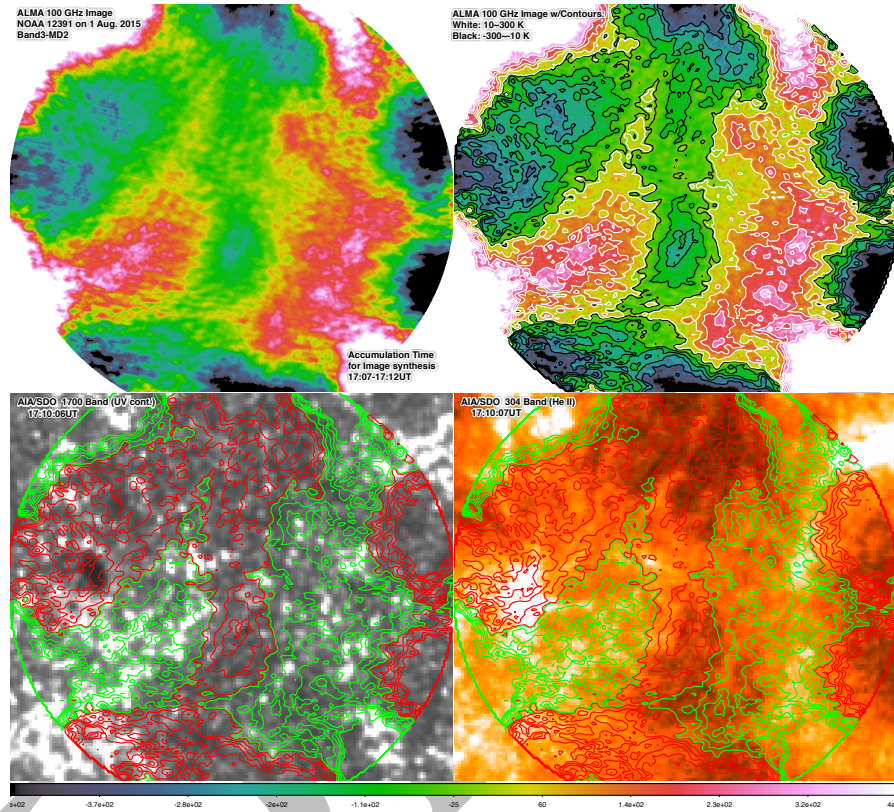


**Figure 3.4:** NOAA12391 observed by ALMA and SDO/AIA. Upper Left: ALMA band 3 image, Upper Right: ALMA band 3 image w/contours, Lower Left: AIA 1700 Å (UV continuum) image w/ALMA contours, and Lower Right: AIA 304 Å (He II) image w/ALMA contours.

#### Example 3: Quiet Sun observed on 11 December 2014

- JIRA ticket: CSV-3167
- Data IDs: uid://A002/X968840/X2aa; uid://A002/X968840/X338
- Band3 and Band6, respectively
- MD mode: MD1 for both

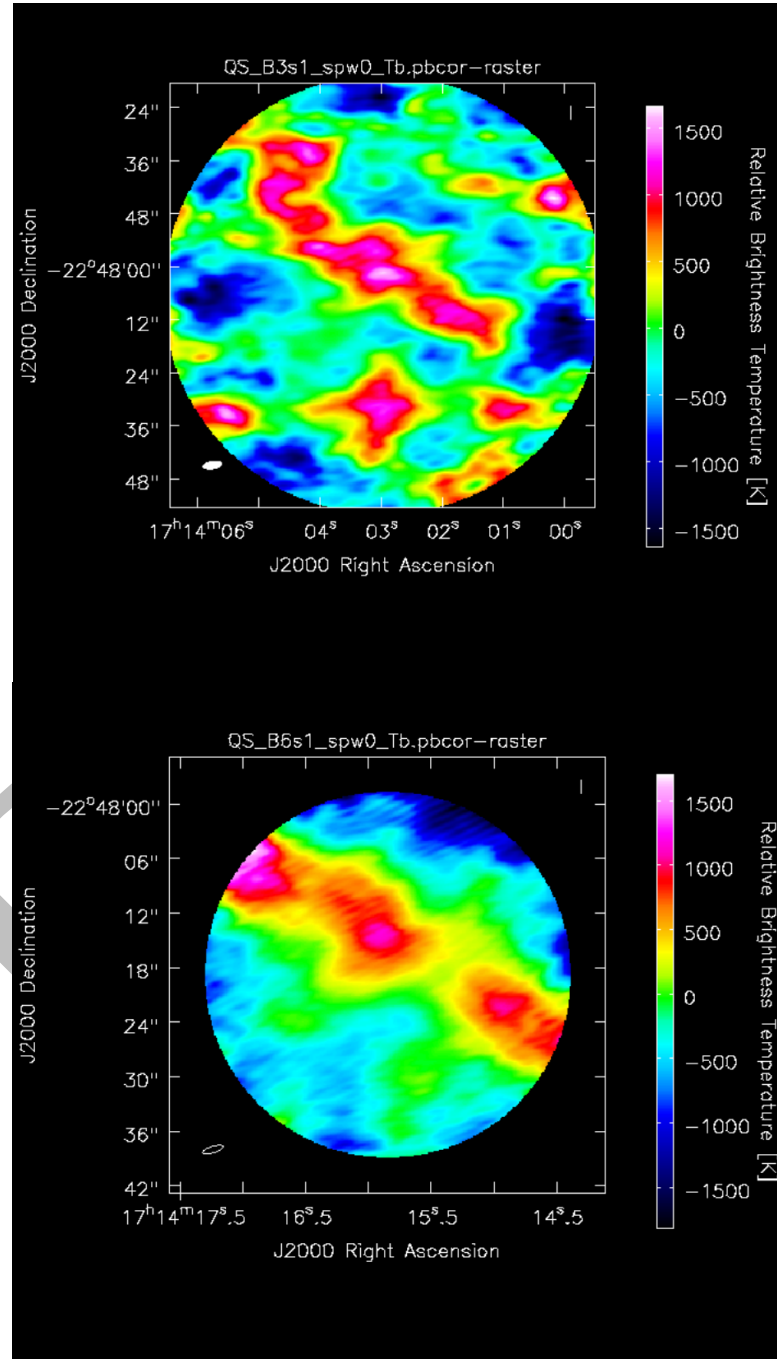


**Figure 3.5:** Quiet Sun observed with ALMA. Upper: Band3. Lower Band6



Example 4: Solar Limb near the north pole on 11 December 2014

- JIRA ticket: CSV-3167
- Data ID: uid://A002/X968840/X117w
- Receiver: Band3
- MD mode: MD1

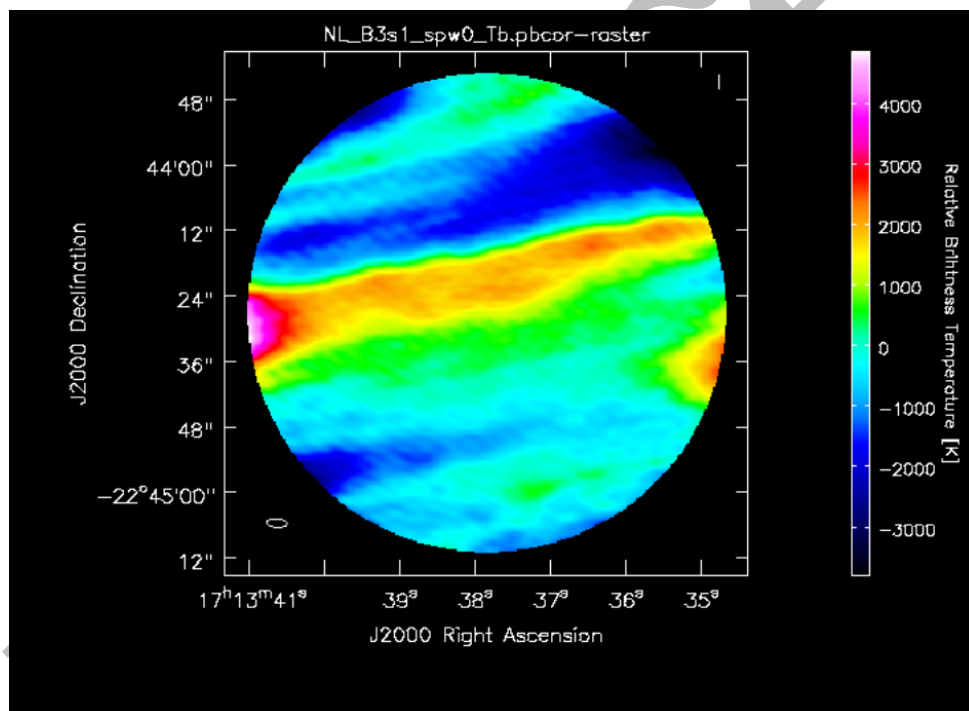


**Figure 3.6:** Solar Limb observed with ALMA Band3-MD1

The solar limb is essentially a “knife edge” compared to the primary beam. The interferometric response is one of strong “overshoot”. Reconstruction of solar limb observations require TP data and will generally involve mosaicking.

### 5.2.2 Pseudo-mosaic example

At the time of the solar observing campaign held in December 2014, the observing script for MOSAIC observations with the MD mode was not yet implemented. We made seven ephemeris files with offset pointings, and carried out a pseudo-mosaic observation using the observing script for single-pointing observations with the MD mode. Although we had to modify the coordinate table in the ASDM dataset manually, we could synthesize a solar image from the pseudo-mosaic data using the CLEAN task of CASA as a proof-of-concept demonstration.

- JIRA ticket: CSV-3167
- Data ID: uid://A002/X971d6b/X1ce
- Receiver: Band3
- MD mode: MD1

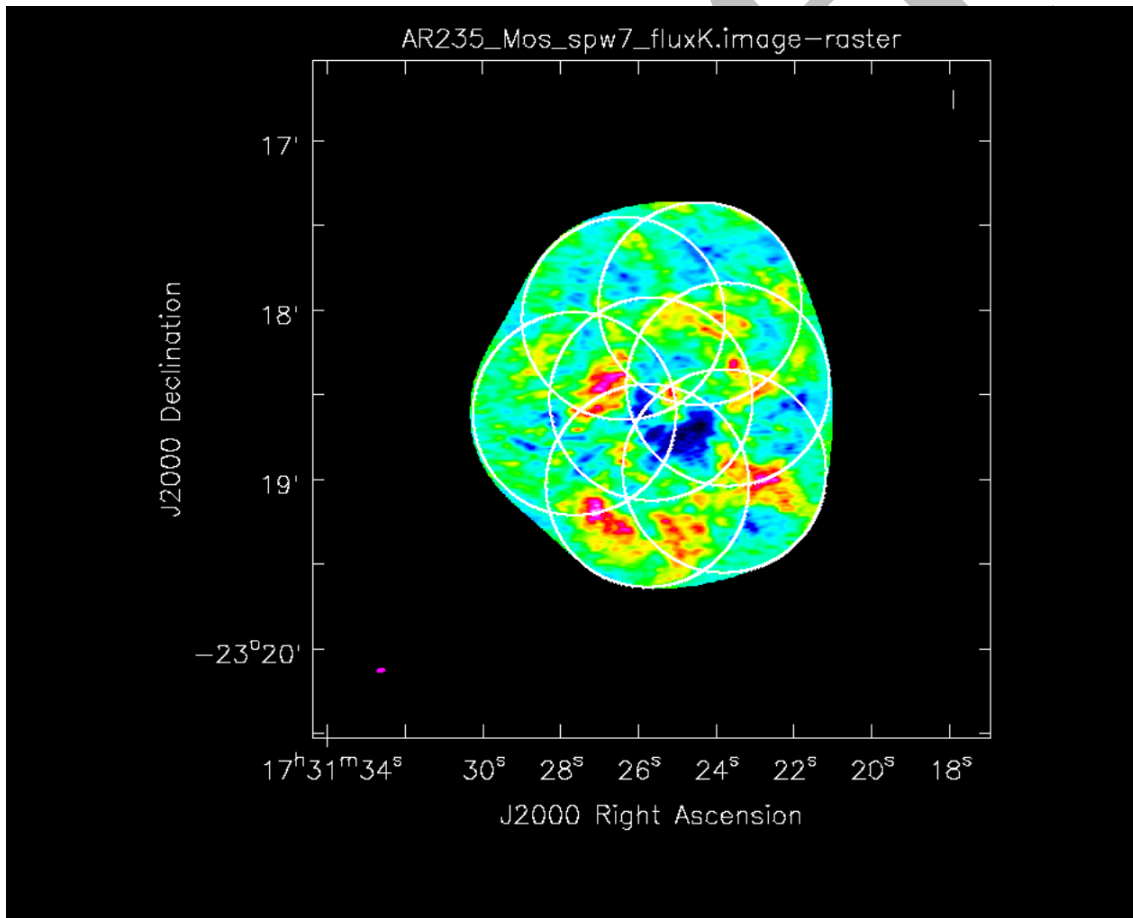


**Figure 3.7:** NOAA12235 synthesized image from with pseudo-mosaic data. White circles indicate 20% levels of the primary beams of the 7 pointings.

Brighter sources are located in the lower part of the map. Counterparts of the brighter sources can be found in the AIA 1700Å images, but the brightness of the sources are similar to other sources, or are indeed darker than the sources located in the middle part

of the map. The inconsistency might not indicate the solar structures in mm wave, but may be caused by our naive assumption that the antenna temperature is constant.

### **5.2.3 Mosaicking**

Since the time of the December 2014 campaign, mosaicking with up to 150 independent pointings relative to an external reference ephemeris became possible (Cycle3-ON). It was superficially demonstrated on 10 July 2015 to the extent that a pointing pattern was executed relative to a reference ephemeris. However, the array was in an extended configuration and was not suitable for imaging the Sun. It is therefore a high priority to test and validate solar mosaicking during the December 2015.

## **6 Solar Observing: Science Operations**

### **6.1 Scheduling Constraints**

Consideration of solar observing campaign(s) in Cycle 4 must allow for constraints imposed by allowed array configurations, shadowing, and antenna tracking performance.

#### **6.1.1 Array Configurations**

Solar images for scientific use are synthesized from a snapshot data, and certainly include large-scale structures. Therefore, snapshot data of a solar observation must have good u-v coverage for large-scale structure. Furthermore, in light of the fact that WVR corrections are not currently available for solar data, compact antenna configurations are favored. Considering the array configurations in Cycle 4, the array configurations C40-1, C40-2, and C40-3 will be used for solar observations. Therefore, the season of the solar observations in Cycle 4 is limited to the period when these configurations are available.

#### **6.1.2 Shadowing**

The 7-m array is essential for solar observations, because the data on short baselines are needed for solar image synthesis to recover large angular scales. To avoid shadowing in the 7m array, we must observe the Sun when the elevation of the Sun is  $>40$  degrees, with margin, implying the following observing periods.

- Summer Solstice [in December]: 13:00~20:00UT (10:00~17:00 CLT)
- Fall/Spring Equinox: 13:30~19:30UT (10:30~16:30 CLT)
- Winter Solstice [in June] 15:30~17:30UT (12:30~15:30 CLT)

#### **6.1.3 Antenna Tracking**

Due to issues with antenna tracking when the source is near the zenith, we cannot observe the Sun near times of the December solstice. If solar observations are carried out in Chilean summer, we may need to suspend solar observations for as much as  $\sim 1$  hr near noon.

## 6.2 Hybrid Antenna Configuration: 7m + 12m

To ensure time synchronization of the data and to obtain good u-v coverage, the heterogeneous array formed from 12m- and 7m-antennas is required for solar observations. That is, all 7m- and 12m-antennas of the array are connected to the Baseline Correlator. The use of the heterogeneous array for solar observations has been validated during the 3<sup>rd</sup>, 4<sup>th</sup>, and 5<sup>th</sup> solar campaigns held in 2012, 2013, and 2014, respectively.

## 6.3 Calibrator Selection

Since the MD mode reduces the sensitivity of the receiver, the criterion for selecting calibrators for non-solar observations cannot be used for solar observations. The flux of phase and flux calibrators has to be  $>1$  Jy with sources  $>2$  Jy preferred. The brightest quasar available will be selected as a bandpass calibrator. As mentioned at section 3., the bandpass calibrator is used to check the soundness of the flux calibration. Therefore; the flux calibrator must not be the same as the bandpass calibrator.

## 6.4 Correlator Mode and Default Observing Frequencies

In contrast to non-solar observations where the observing frequencies can be selected anywhere within the observing frequency range of allowed bands, the observing frequencies for the solar observations in Cycle 4 are restricted to those listed in Table 4.1 because the performance of the MD modes has not been tested and validated across the entire frequency range yet. We do not expect this to be a limitation on the achievable science since solar observations are restricted to continuum (in effect, low spectral resolution) measurements for which the chosen frequencies should be sufficient.

**Table 4.1**

| Band   | LO Freq. | LSB         |             | USB         |             |
|--------|----------|-------------|-------------|-------------|-------------|
|        |          | BB1         | BB2         | BB3         | BB4         |
| Band 3 | 100 GHz  | 92-94 GHz   | 94-96 GHz   | 104-106 GHz | 106-108 GHz |
| Band 6 | 239 GHz  | 229-231 GHz | 231-233 GHz | 245-247 GHz | 247-249 GHz |

Similarly, the baseline correlator mode in Cycle 4 is fixed to the Time Domain Mode (TDM). The Frequency Domain Mode (FDM) may be available in Cycle 5 or beyond.

## 6.5 Solar Scheduling Block

The scheduling block (SB) for solar interferometric observations is developed using the SB that has the project ID is “0000.0.0302CSV”. The observations using this SB were done successfully on 1 August 2015. The antenna configuration was C34-5 at that time, and it is not suitable for solar image synthesis because the data of short baselines are not enough. Hence, the solar images synthesized from the observing data in August do not have quality enough for verifying solar images that will be obtained in Cycle4.

For reference, an example of the observing sequence is shown as follows.

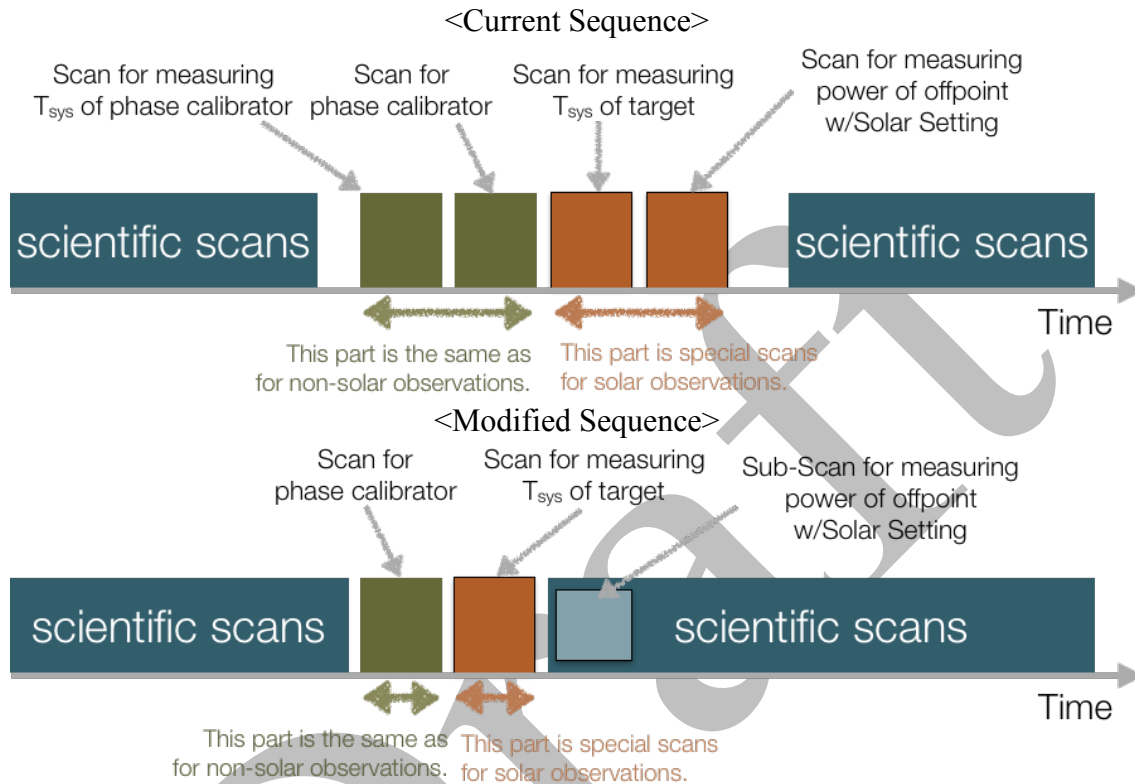
The observing sequence of the interferometric observations executed on 1 August 2015

- Receiver: Band3
- MD mode: MD2
- Bandpass/Sideband calibrator: J1058+0133
- Flux calibrator: J0255-3627
- Phase calibrator: J0854+2006
- Data ID: uid://A002/Xa72fea/Xd96

| ID | Time (UT)                  | Target     | ATT | Intent          | Comment                                 |
|----|----------------------------|------------|-----|-----------------|---|
| 1  | 16:36:40.9 -<br>16:37:45.2 | Sun        | –   | Atm. Cal.       | For measuring $P_{\text{zero}}$         |
| 2  | 16:38:32.6 -<br>16:40:27.7 | J1058+0133 | –   | Pointing Cal.   |   |
| 3  | 16:41:29.6 -<br>16:42:32.2 | J1058+0133 | –   | Sideband Cal.   |   |
| 4  | 16:43:35.6 -<br>16:43:51.7 | J1058+0133 | –   | Atm. Cal.       |   |
| 5  | 16:44:52.8 -<br>16:50:09.3 | J1058+0133 | Sun | Bandpass Cal.   |   |
| 6  | 16:51:17.6 -<br>16:53:12.7 | J0255-3627 | –   | Pointing Cal.   |   |
| 7  | 16:54:12.7 -<br>16:54:28.9 | J0255-3627 | –   | Atm. Cal.       |   |
| 8  | 16:55:28.3 -<br>16:58:05.6 | J0255-3627 | Red | Flux Cal.       |   |
| 9  | 16:59:05.3 -<br>17:01:00.2 | J0854+2006 | –   | Pointing Cal.   |   |
| 10 | 17:02:01.3 -<br>17:02:17.4 | J0854+2006 | –   | Atm. Cal.       |   |
| 11 | 17:03:13.0 -<br>17:03:43.3 | J0854+2006 | Red | Phase Cal.      |   |
| 12 | 17:04:42.8 -<br>17:04:59.4 | Sun        | –   | Atm. Cal.       | For measuring $P_{\text{hot/cold/sky}}$ |
| 13 | 17:06:01.1 -<br>17:06:17.5 | Sun        | Sun | Atm. Cal.       | For measuring $P_{\text{off}}$          |
| 14 | 17:07:17.2 -<br>17:12:49.3 | Sun        | Sun | Scientific Obs. |   |
| 15 | 17:13:52.9 -<br>17:14:09.1 | J0854+2006 | –   | Atm. Cal.       |   |
| 16 | 17:15:04.8 -<br>17:15:35.0 | J0854+2006 | Red | Phase Cal.      |   |

- “ATT” indicates the setting of the attenuators in IFswitch and IFprocessor.
  - Sun: The attenuation levels optimized for the science target (Sun). The optimization was carried out before Scan ID 1.
  - Red: The attenuation levels are reduced from the “Sun” along the following values: IFswitch: - 7dB / For IFprocessor: 0dB.

In the current observing sequence, the duration of the phase & amplitude calibration between scientific scans is over 5 minutes, and the significant interruption between scientific scans may cause an unacceptable impact to solar science objectives. To reduce the duration, we plan to modify the SB as follows.



With this modification, the duration of the calibration can be reduced to less than 3 minutes. The observing sequence will be verified during the solar campaign in December 2015.

## 6.6 Single-dish observing

As described above, the single dish observing sequence is relatively straightforward. The calibration power measurements are included in the basic script used for fast-scan mapping, *FastScanObs\_md.py*. In addition, standard pointing and focus scans on a suitable source are used to optimize telescope performance prior to fast-scan mapping. We plan to use one PM dish for regular sky-dips to track atmospheric opacity, and the remaining PM dishes (more than one, for redundancy and in case of problems) will be executing repeated fast-scan maps in conjunction with the interferometer observations.

## **7 2015 Solar Observing Campaign**

The 2015 Solar Observing Campaign took place from 14-22 December 2015, just before the end of this study. Its primary purpose was to serve as a “dress rehearsal” of ALMA Cycle 4 solar observing capabilities. In this, it succeeded.

The team also intended to do preliminary testing of anticipated Cycle 5 capabilities, including, but not restricted to:

- Determine MD1 and MD2 settings for bands 7 and 9
- Determine IF Switch and IF Proc settings in bands 7 and 9
- Check calibration transfer in bands 7 and 9
- Observe in subarrays
- Execute fast-scan mapping of subregions at high cadence
- Observe in spectral line mode (radio recombination lines and possibly CO)

Unfortunately, observations on most days were cut short by high winds in the afternoon. Priority was given to Cycle 4 capabilities in the morning and therefore potential Cycle 5 capabilities, planned for afternoons, were not achieved for the most part. The one exception was the first bullet above. We were able to establish voltage bias settings for MD1 and MD2 in bands 7 and 9. We are currently planning tests to address the remaining bullets in March and April in advance of the Cycle 5 “modes meeting” at the end of April.

## **8 Outreach Activities**

As summarized in the Introduction, the activities summarized in Sections 2-7 were accompanied by extensive outreach to the solar community. We briefly outline each of these below.

### **8.1 Meetings and Workshops**

Members of the development team presented contributed and invited talks, as well as numerous posters, at a large number of professional meetings and workshops:

- 31<sup>st</sup> URSI GASS, August 2014, Beijing, China
- 14<sup>th</sup> ESPM Meeting, September 2014, Dublin, Ireland
- NASA LWS Workshop on Evolving Solar Activity and its Influence on Space and Earth, November 2014, Portland, OR
- Revolution in Astronomy with ALMA: the Third Year, December 2014, Tokyo, Japan
- AAS, January 2015, Seattle, WA
- Measurement Techniques for Solar and Space Physics, April 2015, Boulder, CO



- AAS TESS meeting, May 2015, Indianapolis, IN
- IRIS 4 Workshop, May 2015, Boulder, CO
- IUGG/IGA meeting, June-July 2015, Prague, Czech Rep.
- 14<sup>th</sup> RHESSI Workshop, August 2015, Owens Valley, CA
- Hinode 9 meeting, September 2015, Belfast, Ireland
- Ground-based Solar Observations in the Space Instrumentation Era, October 2015, Coimbra, Portugal
- IAU GA, August 2015, Honolulu, HI

## 8.2 Proceeding Publications

Many, but by no means all, meetings led to proceedings publications:

- Wedemeyer, S., and 36 colleagues 2016 “ALMA Observations of the Sun in Cycle 4 and Beyond”, *ArXiv e-prints arXiv:1601.00587*.
- Phillips, N., Hills, R., Bastian, T., Hudson, H., Marson, R., Wedemeyer, S. 2015 “Fast Single-Dish Scans of the Sun Using ALMA”, *Revolution in Astronomy with ALMA: The Third Year* 499, 347.
- Wedemeyer, S., Bastian, T., Brajsa, R., Barta, M., Shimojo, M., Hales, A., Yagoubov, P., Hudson, H. 2015, “Solar ALMA Observations - A New View of Our Host Star”, *Revolution in Astronomy with ALMA: The Third Year* 499, 345.
- Wedemeyer, S., Bastian, T., Brajsa, R., Barta, M., Shimojo, M. 2015, “Solar Simulations for the Atacama Large Millimeter Observatory Network”, *Revolution in Astronomy with ALMA: The Third Year* 499, 341.
- Wedemeyer, S., and 28 colleagues 2015, “SSALMON - The Solar Simulations for the Atacama Large Millimeter Observatory Network”, *Advances in Space Research* 56, 2679-2692.
- Wedemeyer, S., Bastian, T. S., Brajsa, R., Barta, M. 2015, “SSALMON - The Solar Simulations for the Atacama Large Millimeter Observatory Network”, *IAU General Assembly 22*, 2257466.
- Bastian, T.S., and 14 colleagues 2015, “The Atacama Large Millimeter/Submillimeter Array: a New Asset for Solar and Heliospheric Physics”, *IAU General Assembly 22*, 2257295.
- Wedemeyer, S., Brajsa, R., Bastian, T. S., Barta, M., Hales, A., Yagoubov, P., Hudson, H., Loukitcheva, M., Fleishman, G. 2015, “Solar ALMA observations - A revolutionizing new view at our host star”, *IAU General Assembly 22*, 2256732.
- Bastian, T. S. 2015, “Solar Observations with the Atacama Large Millimeter/submillimeter Array (ALMA)”, *AAS/AGU Triennial Earth-Sun Summit 1*, 203.23.
- Bastian, T. S., Shimojo, M., Wedemeyer-Bohm, S., & ALMA North American Solar Development Team, 2015 “Observing the Sun with ALMA: A New

### 8.3 Science Review

A major effort, led by team member Sven Wedemeyer, was to marshal the collective efforts of nearly 40 scientists to prepare a review paper detailing the broad science that ALMA is positioned to address in the coming years. The result was a review paper published by *Space Science Reviews* late in 2015 that is sure to serve as a reference.

### 8.4 ALMA Science Simulations Group: SSALMON

Wedemeyer also took the lead in organizing an group of nearly 80 scientists to identify science questions that would benefit from detailed numerical simulations using sophisticated MHD codes: “Solar Simulations for the Atacama Large Millimeter Observatory Network (SSALMON; see <http://www.ssalmom.uio.no/>). The group regularly publishes a newsletter.

### 8.5 Synergies

The team reached out to other sectors of the scientific community to ensure scientific engagement and to maximize science return from Cycle 4 solar observing and beyond.

First, beginning with the December 2014 campaign and again with the December 2015 campaign, we enlisted supporting observations from the NASA IRIS and Hinode missions, and from ground based telescopes at Big Bear Solar Observatory and Cerro Tololo. This allowed us to not only obtain valuable context observations for our campaigns, but to also establish a working operational relationship with other observatories.

Second, we have organized an international workshop to be hosted by the National Solar Observatory in Boulder, CO, on March 15-18, 2016. It will be held jointly with user communities for the DKIST O/IR telescope, due to see first light in 2019, and the NASA IRIS mission, which studies the chromosphere in UV wavelengths. We expect about 80 attendees. The meeting also includes an “NRAO Live” event to give tutorials on radio interferometry, the ALMA OT, and related issues. Finally, side meetings are being organized to

- Discuss continuing efforts to enable enhanced solar observing modes on ALMA
- Discuss the release of solar ALMA CSV data to the public
- Identify science objectives and proposing teams for Cycle 4

Finally, the development team has reached out to the stellar community to explore scientific issues of mutual interest. The next Cool Stars meeting in Upsala, June 2016, will include a session on ALMA and the Sun. The team has also proposed a team for the International Space Science Institute in Bern, Switzerland, to consider the solar-stellar connection through the ALMA lens.

## **9 Concluding Remarks**

The ALMA Development Study served as an important catalyst to bring ALMA solar observing modes forward and to introduce these exciting new capabilities to the solar physics community – as well as the stellar community. Much work remains to be done – to prepare and execute proposals in Cycle 4 and to continue bringing new capabilities online in future observing cycles. Nevertheless, the capabilities offered in Cycle 4 are an excellent beginning.

## **Acknowledgments**

We convey special thanks to Pavel Yagoubov for suggesting and testing the MD modes; to Tony Remijan, Antonio Hales, Akihiko Hirota, and Neil Phillips for their excellent support of the 2014 solar observing campaign and EOC testing; to Richard Hills for broad input on a range of relevant topics and for his leadership in developing the fast-scanning mode; and to Sven Wedeymeyer for his leadership in developing the ALMA science review and for organizing the SSALMON group. We additionally thank the following individuals for their efforts in supporting ALMA solar development, listed alphabetically: Miro Barta, Roman Brajsa, Bin Chen, Dale Gary, Gregory Fleishman, Hugh Hudson, Gordon Hurford, Adam Kobelski, Maria Loukitcheva, Sām Krucker, Ivica Skokic, and Yihua Yan. Finally we thank the NSF for its support of the ALMA solar development study entitled “Advanced Solar Observing Techniques” (Bastian, PI) and ESO for its support of the companion study entitled “Solar Research with ALMA” (Brajsa, PI).

## Appendix A

Following below is the CASA script use to calibrate and image solar single-dish data. This version of the script produces separate images for each antenna, polarization and IF sideband.

```
# inputs
src='sun'
ants=["PM02","PM04"]
baseuid='./Band6_Sun_norm/uid___A002_X9ea048_X1c3'
base='X1c3'

# import the ASDM file and create a measurement set
importasdm(asdm=baseuid,with_pointing_correction=True,verbose=True,
vis=base+'.ms',applyflags=False,bdfflags=True,overwrite=True)

# list contents of file:
scans = sd.scantable(base+'.ms', average=False)
scans.summary(filename=base+'.summary')

# split into files for each antenna
sdsave(infile=base+'.ms',outform='ASAP',outfile=base+'.asap',
overwrite=True,splitant=True)

# calibrate each antenna:
for ant in ants:
    sdcal2(base+'.'+ant+'.asap',calmode='otf,tsys,apply',tsysspw='0,1,2,3',
    spwmap={0:[0],1:[1],2:[2],3:[3]},fraction='20%',
    outfile=base+'.'+ant+'.asap.cal')
    sdsave(infile=base+'.'+ant+'.asap.cal',outform='MS2',
    outfile=base+'.'+ant+'.asap.cal.ms')

# map each antenna, pol and IF sideband, image parameters for Band 6:
for ant in ants:
    for pol in ['XX', 'YY']:
        for spw in ['0', '1', '2', '3']:
            sdimage(infiles=base+'.'+ant+'.asap.cal.ms',spw=spw,nchan=1,
            cell=['3.0arcsec','3.0arcsec'],imsize=[1000,1000],
            outfile=base+'.'+ant+'.pol'+pol+'.spw'+spw+'.im',
            gridfunction='GAUSS',gwidth='6arcsec',stokes=pol,
            ephemsrname=src)
            exportfits(imagename=base+'.'+ant+'.pol'+pol+'.spw'+spw+'.im',
            fitsimage=src+'_'+base+'_'+ant+'_'+pol+'_'+spw+'.fits')
```

## Appendix B

Following below is the python script use to calibrate solar interferometer data.

```
# JIRA ticket: CSV-3204
# TARGET: Sunspot in NOAA12391 (Ephemeris)
# Data ID: uid://A002/Xa72fea/Xd96
# CASA Version for the script: CASA Version 4.4.0

# ALMA Data Reduction Script
# Calibration

#Switch for each process
thesteps = []
step_title = {0: 'Import of the ASDM',
              1: 'listobs & Ant_config',
              2: 'Fix of SYSCAL table times',
              3: 'Calculate Antenna Temperatures from QLSD',
              4: 'A priori flagging',
              5: 'Generation of the Tsys cal tables',
              6: 'Application of Tsys table to the calibraots',
              7: 'Split out science SPWs',
              8: 'Listobs, and save original flags',
              9: 'Initial flagging',
              10: 'Putting a model for the flux calibrator(s)',
              11: 'Save flags before bandpass cal',
              12: 'Bandpass calibration',
              13: 'Save flags before gain cal',
              14: 'Gain calibration',
              15: 'Save flags before applycal',
              16: 'Application of the bandpass and gain cal tables',
              17: 'Split out corrected column',
              18: 'Save flags after applycal'}

##### Comment from MS: You need to execute step 3,4,5 at the same time.

# The Python variable 'mysteps' will control which steps
# are executed when you start the script using
#   execfile('scriptForCalibration.py')
# e.g. setting
#   mysteps = [2,3,4]# before starting the script will make the script execute
# only steps 2, 3, and 4
# Setting mysteps = [] will make it execute all steps.

#=====
#ASDM Directory Name
asdm ='uid__A002_Xa72fea_Xd96'

# scan and spw for calculation of antenna temperature
zscan = 1 # Scan For Pzero
```

```

ascan = 12 # Scan For Psky/amb/hot
sscan = 13 # Scan For Poff
oscan = '14' # Scan For Sun (Target)
ospw = '0,1,2,3' # spw for hot/amb/sky
zspw = '13,14,15,16' # spw for off
sspw = [5,7,9,11] # spw for scientific obs.

# Data Name & Image Name
mso = asdm + '.ms'
mss = asdm + '_split.ms'
zms = asdm + '_Pzer.ms'
oms = asdm + '_Poff.ms'
ams = asdm + '_Pamb.ms'
hms = asdm + '_Phot.ms'
sms = asdm + '_Psky.ms'
ads = asdm + '_Pamd.ms'
sun = asdm + '_Psun.ms'
csv_file = asdm + '_Tant.csv'

import analysisUtils as au
import csv
=====

import re
import os

if 'applyonly' not in globals(): applyonly = False
try:
    print 'List of steps to be executed ...', mysteps
    thesteps = mysteps
except:
    print 'global variable mysteps not set.'
if (thesteps==[]):
    thesteps = range(0,len(step_title))
    print 'Executing all steps: ', thesteps

if applyonly != True: es = aU.stuffForScienceDataReduction()

if re.search('^4.4.0', casadef.casa_version) == None:
    sys.exit('ERROR: PLEASE USE THE SAME VERSION OF CASA THAT YOU USED FOR
    GENERATING THE SCRIPT: 4.4.0')

# CALIBRATE_ATMOSPHERE: Sun(Active Region w/Sunspot) J1058+0133 J0522-3627
J0854+2006
# CALIBRATE_BANDPASS: J1058+0133
# CALIBRATE_FLUX: J0522-3627
# CALIBRATE_PHASE: J0854+2006
# CALIBRATE_POINTING: J1058+0133 J0522-3627 J0854+2006
# OBSERVE_TARGET: Sun(Active Region w/Sunspot)

# Using reference antenna = PM03

```

```

# Import of the ASDM
mystep = 0
if(mystep in thesteps):
    casalog.post('Step '+str(mystep)+' '+step_title[mystep],'INFO')
    print 'Step ', mystep, step_title[mystep]

=====

if os.path.exists(mso) == False:
    importasdm(asdm = asdm, vis = mso,
        asis='Antenna Station Receiver Source CalAtmosphere CalWVR CorrelatorMode
SBSummary CalDevice ')
===== (added CalDevice to asis)

# listobs
mystep = 1
if(mystep in thesteps):
    casalog.post('Step '+str(mystep)+' '+step_title[mystep],'INFO')
    print 'Step ', mystep, step_title[mystep]

#dump of the observing information
os.system('rm -rf'+ asdm + '_listobs.txt')
listobs(mso, listfile = asdm + '_listobs.txt')

#make the plot of the antenna configuration
os.system('rm -rf'+ asdm + '_antconf.png')
plotants(mso, figfile= asdm + '_antconf.png')

=====

es.listobs3(mso,figfile='listobs3_int.png')

=====

# Fix of SYSCAL table times
mystep = 2
if(mystep in thesteps):
    casalog.post('Step '+str(mystep)+' '+step_title[mystep],'INFO')
    print 'Step ', mystep, step_title[mystep]

from recipes.almahelpers import fixsyscaltimes
fixsyscaltimes(vis = mso)

=====

#Calculaion of Antenna Temperature from QLSD
mystep = 3
if(mystep in thesteps):
    casalog.post('Step '+str(mystep)+' '+step_title[mystep],'INFO')
    print 'Step ', mystep, step_title[mystep]

tb.open('%s/ANTENNA' % mso)

```



```

antnames = tb.getcol('NAME')
tb.close()

flagdata(vis = mso,
         mode = 'manual',
         timerange = '2015/08/01/17:07:15 ~ 2015/08/01/17:07:30',
         flagbackup = F)

flagdata(vis = mso,
         mode = 'manual',
         timerange = '2015/08/01/17:12:40 ~ 2015/08/01/17:12:50',
         flagbackup = F)

#---
SubInf = au.computeDurationOfScan(zscan, vis=mso, returnSubscanTimes=True)

#P_zero
os.system('rm -rf' + zms)
split(vis = mso,
      outputvis = zms,
      timerange = SubInf[3][2],
      datacolumn = 'data',
      spw = zspw,
      timebin = '125s')

tb.open(zms)
PzTbl = {}
for i in range(0, len(antnames)):
    sel = tb.query('ANTENNA1==%d' % i)
    zd = sel.getcol('DATA')
    PzTbl[antnames[i]] = zd
tb.close()

#----
SubInf = au.computeDurationOfScan(ascan, vis=mso, returnSubscanTimes=True)

#P_sky
os.system('rm -rf' + sms)
split(vis = mso,
      outputvis = sms,
      timerange = SubInf[3][1],
      datacolumn = 'data',
      spw = ospw,
      timebin = '125s')

tb.open(sms)
PsTbl = {}
for i in range(0, len(antnames)):
    sel = tb.query('ANTENNA1==%d' % i)
    zd = sel.getcol('DATA')
    PsTbl[antnames[i]] = zd
tb.close()

```

```
#P_amb(cold)
```

```
os.system('rm -rf' + ams)
```

```
split(vis = mso,  
      outputvis = ams,  
      timerange = SubInf[3][2],  
      datacolumn = 'data',  
      spw = ospw,  
      timebin = '125s')
```

```
tb.open(ams)
```

```
PaTbl = {}
```

```
for i in range(0, len(antnames)):  
    sel = tb.query('ANTENNA1==%d' % i)  
    zd = sel.getcol('DATA')  
    PaTbl[antnames[i]] = zd  
tb.close()
```

```
#P_hot
```

```
os.system('rm -rf' + hms)
```

```
split(vis = mso,  
      outputvis = hms,  
      timerange = SubInf[3][3],  
      datacolumn = 'data',  
      spw = ospw,  
      timebin = '125s')
```

```
tb.open(hms)
```

```
PhTbl = {}
```

```
for i in range(0, len(antnames)):  
    sel = tb.query('ANTENNA1==%d' % i)  
    zd = sel.getcol('DATA')  
    PhTbl[antnames[i]] = zd  
tb.close()
```

```
#Temperature of hot / amb loads
```

```
TLoad = au.getLoadTemperatures(mso, doplot=False, warnIfNoLoadTemperatures=True)
```

```
SubInf = au.computeDurationOfScan(sscan, vis=mso, returnSubscanTimes=True)
```

```
#P_off
```

```
os.system('rm -rf' + oms)
```

```
split(vis = mso,  
      outputvis = oms,  
      timerange = SubInf[3][1],  
      datacolumn = 'data',  
      spw = ospw,  
      timebin = '125s')
```

```
tb.open(oms)
```

```

PoTbl = {}
for i in range(0, len(antnames)):
    sel = tb.query('ANTENNA1==%d' % i)
    zd = sel.getcol('DATA')
    PoTbl[antnames[i]] = zd
tb.close()

#P_sun
os.system('rm -rf' + sun)
split(vis = mso,
      scan = oscan,
      outputvis = sun,
      datacolumn = 'data',
      spw = ospw,
      timebin = '800s')

tb.open(sun)
PsunTbl = {}
for i in range(0, len(antnames)):
    sel = tb.query('ANTENNA1==%d' % i)
    zd = sel.getcol('DATA')
    PsunTbl[antnames[i]] = zd
tb.close()

#Calculation of T_ant

Tant = {}
for ant in antnames:
    for pol in range(0,2):
        tantt = []
        for spw in range(0,4):

            sunv = PsunTbl[ant][pol][0][spw].real
            zv = PzTbl[ant][pol][0][spw].real
            if zv < 0: zv = 0
            ov = PoTbl[ant][pol][0][spw].real
            sv = PsTbl[ant][pol][0][spw].real
            hv = PhTbl[ant][pol][0][spw].real
            av = PaTbl[ant][pol][0][spw].real
            at = TLoad[ant][ascan]['amb']
            ht = TLoad[ant][ascan]['hot']

            tantt.append(((sunv-zv)*(sv-zv)*(ht-at)/((ov-zv)*(hv-av))))

        if pol == 0:
            Tant[ant] = {'XX': tantt, 'YY': tantt}
        else:
            Tant[ant]['YY'] = tantt

#Create a CSV file of T_ant
os.system('rm -rf' + csv_file)

```

```

csv_table=[]
csv_tcolumn = ['Ant',
                'BB1/Tant:XX','BB1/Tant:YY',
                'BB2/Tant:XX','BB2/Tant:YY',
                'BB3/Tant:XX','BB3/Tant:YY',
                'BB4/Tant:XX','BB4/Tant:YY',
                'BB1/Pzero:XX','BB1/Pzero:YY',
                'BB2/Pzero:XX','BB2/Pzero:YY',
                'BB3/Pzero:XX','BB3/Pzero:YY',
                'BB4/Pzero:XX','BB4/Pzero:YY',
                'BB1/Poff:XX','BB1/Poff:YY',
                'BB2/Poff:XX','BB2/Poff:YY',
                'BB3/Poff:XX','BB3/Poff:YY',
                'BB4/Poff:XX','BB4/Poff:YY',
                'BB1/Psky:XX','BB1/Psky:YY',
                'BB2/Psky:XX','BB2/Psky:YY',
                'BB3/Psky:XX','BB3/Psky:YY',
                'BB4/Psky:XX','BB4/Psky:YY']

```

```

csv_table.append(csv_tcolumn)

```

```

for ant in antnames:

```

```

    csv_column = []
    csv_column.append(ant)
    csv_column.append(Tant[ant]['XX'][0])
    csv_column.append(Tant[ant]['YY'][0])
    csv_column.append(Tant[ant]['XX'][1])
    csv_column.append(Tant[ant]['YY'][1])
    csv_column.append(Tant[ant]['XX'][2])
    csv_column.append(Tant[ant]['YY'][2])
    csv_column.append(Tant[ant]['XX'][3])
    csv_column.append(Tant[ant]['YY'][3])
    csv_column.append(PzTbl[ant][0][0][0].real)
    csv_column.append(PzTbl[ant][1][0][0].real)
    csv_column.append(PzTbl[ant][0][0][1].real)
    csv_column.append(PzTbl[ant][1][0][1].real)
    csv_column.append(PzTbl[ant][0][0][2].real)
    csv_column.append(PzTbl[ant][1][0][2].real)
    csv_column.append(PzTbl[ant][0][0][3].real)
    csv_column.append(PzTbl[ant][1][0][3].real)
    csv_column.append(PoTbl[ant][0][0][0].real)
    csv_column.append(PoTbl[ant][1][0][0].real)
    csv_column.append(PoTbl[ant][0][0][1].real)
    csv_column.append(PoTbl[ant][1][0][1].real)
    csv_column.append(PoTbl[ant][0][0][2].real)
    csv_column.append(PoTbl[ant][1][0][2].real)
    csv_column.append(PoTbl[ant][0][0][3].real)
    csv_column.append(PoTbl[ant][1][0][3].real)
    csv_column.append(PsTbl[ant][0][0][0].real)
    csv_column.append(PsTbl[ant][1][0][0].real)
    csv_column.append(PsTbl[ant][0][0][1].real)

```

```

csv_column.append(PsTbl[ant][1][0][1].real)
csv_column.append(PsTbl[ant][0][0][2].real)
csv_column.append(PsTbl[ant][1][0][2].real)
csv_column.append(PsTbl[ant][0][0][3].real)
csv_column.append(PsTbl[ant][1][0][3].real)
csv_table.append(csv_column)

with open (csv_file, 'wb') as f:
    tantsys = csv.writer(f)
    tantsys.writerows(csv_table)
=====

# A priori flagging
mystep = 4
if(mystep in thesteps):
    casalog.post('Step '+str(mystep)+' '+step_title[mystep], 'INFO')
    print 'Step ', mystep, step_title[mystep]

flagdata(vis = mso,
         mode = 'manual',
         intent = '*POINTING*,*SIDEBAND_RATIO*,*ATMOSPHERE*',
         flagbackup = F)

flagdata(vis = mso,
         mode = 'manual',
         autocorr = T,
         flagbackup = F)

flagdata(vis = mso,
         mode = 'manual',
         spw = '0~4',
         autocorr = T,
         flagbackup = F)

flagdata(vis = mso,
         mode = 'manual',
         spw = '6,8,10',
         autocorr = T,
         flagbackup = F)

flagdata(vis = mso,
         mode = 'manual',
         spw = '12~36',
         autocorr = T,
         flagbackup = F)

flagcmd(vis = mso,
        inpmode = 'table',
        useapplied = True,
        action = 'plot',
        plotfile = mso+'.flagcmd.png')

```

```

flagcmd(vis = mso,
        inpmode = 'table',
        useapplied = True,
        action = 'apply')

flagmanager(vis = mso,
            mode = 'save',
            versionname = 'priori')

#Make Tsys table and Apply for calibrators.
mystep = 5
if(mystep in thesteps):
    casalog.post('Step '+str(mystep)+' '+step_title[mystep],'INFO')
    print 'Step ', mystep, step_title[mystep]

    os.system('rm -rf' + mso + '.tsys')
    os.system('rm -rf' + mso + '.tsys_org')
    gencal(vis = mso, caltable = mso + '.tsys', caltype = 'tsys')

# Flagging edge channels
flagdata(vis = mso + '.tsys',
        mode = 'manual',
        spw = '5:0~9;116~127,7:0~9;116~127,9:0~9;116~127,11:0~9;116~127',
        flagbackup = F)

=====
flagdata(vis = mso + '.tsys',
        mode = 'manual',
        scan='1,13',
        flagbackup = F)

#Added antenna temperature
os.system('cp -r' + mso + '.tsys' +mso+'.tsys_org')
polxy = ['XX','YY']
for i in range(0, len(antnames)):
    for spw in range(0, len(sspw)):
        tb.open(mso + '.tsys', nomodify = F)
        sel = tb.query('ANTENNA1==%d && SCAN_NUMBER==%d &&
SPECTRAL_WINDOW_ID==%d' % (i, ascan, sspw[spw]))
        tsyst = sel.getcol("FPARAM")
        tantt = tsyst
        tsflag = sel.getcol("FLAG")
        for pol in range(0, tsyst.shape[0]):
            Sun_Tant = Tant[antnames[i]][polxy[pol]][spw]
            for ch in range(0, tsyst.shape[1]):
                if tsflag[pol, ch, 0] == F:
                    tantt[pol, ch, 0] = tsyst[pol, ch, 0] + Sun_Tant
            sel.putcol("FPARAM", tantt)
        tb.close()

```

```

#Remove scan for P_zero and P_off
tb.open(mso + '.tsys', nomodify = F)
sel = tb.query('SCAN_NUMBER==%d' % zscan)
zrows = sel.rownumbers()
tb.removeverrows(zrows)
tb.close

tb.open(mso + '.tsys', nomodify = F)
sel = tb.query('SCAN_NUMBER==%d' % sscan)
srows = sel.rownumbers()
tb.removeverrows(srows)
tb.close()
#=====

if applyonly != True:
    au.plotbandpass(caltable=mso+'.tsys', overlay='time',
                    xaxis='freq', yaxis='amp', subplot=22, buildpdf=False, interactive=False,
                    showatm=True, pwv='auto', chanrange='92.1875%', showfdm=True,
showBasebandNumber=True,
                    field="", figfile=mso+'.tsys.plots.overlayTime/'+mso+'.tsys')

if applyonly != True:
    es.checkCalTable(mso+'.tsys', msName=mso, interactive=False)

#Application of Tsys table to the calibraots
mystep = 6
if(mystep in thesteps):
    casalog.post('Step '+str(mystep)+' '+step_title[mystep], 'INFO')
    print 'Step ', mystep, step_title[mystep]

# from recipes.almahelpers import tsysspwmap
# tsysmap = tsysspwmap(vis = mso, tsystable = mso+'.tsys', tsysChanTol = 1)

# Apply to Sun
applycal(vis = mso,
        field = '0',
        spw = '5,7,9,11',
        scan = '14',
        gaintable = mso + '.tsys',
        gainfield = '0',
        interp = 'linear,linear',
#         spwmap = tsysmap,
        calwt = T,
        flagbackup = F)

# Apply to Bandpass Calibrator
applycal(vis = mso,
        field = '1',
        spw = '5,7,9,11',
        gaintable = mso + '.tsys',

```

```

        gainfield = '1',
        interp = 'linear,linear',
#         spwmap = tsysmap,
        calwt = T,
        flagbackup = F)

# Apply to Amplitude Calibrator
applycal(vis = mso,
        field = '2',
        spw = '5,7,9,11',
        gaintable = mso + '.tsys',
        gainfield = '2',
        interp = 'linear,linear',
#         spwmap = tsysmap,
        calwt = T,
        flagbackup = F)

# Apply to Phase Calibrator
applycal(vis = mso,
        field = '3',
        spw = '5,7,9,11',
        gaintable = mso + '.tsys',
        gainfield = '3',
        interp = 'linear,linear',
#         spwmap = tsysmap,
        calwt = T,
        flagbackup = F)

if applyonly != True: es.getCalWeightStats(mso)

# Split out science SPWs and time average
mystep = 7
if(mystep in thesteps):
    casalog.post('Step '+str(mystep)+' '+step_title[mystep], 'INFO')
    print 'Step ', mystep, step_title[mystep]

os.system('rm -rf' + mss)
os.system('rm -rf' + mss + '.flagversions')
split(vis = mso,
        outputvis = mss,
        datacolumn = 'corrected',
        scan = '5,8,11,14,16',
        spw = '5,7,9,11',
        keepflags = T)

# Listobs, and save original flags
mystep = 8
if(mystep in thesteps):
    casalog.post('Step '+str(mystep)+' '+step_title[mystep], 'INFO')
    print 'Step ', mystep, step_title[mystep]

```



```

os.system('rm -rf' + mss+ '.listobs.txt')
listobs(vis = mss,
        listfile = mss + '.listobs.txt')

if not os.path.exists(mss + '.flagversions/Original.flags'):
    flagmanager(vis = mss,
                mode = 'save',
                versionname = 'Original')

# Initial flagging
mystep = 9
if(mystep in thesteps):
    casalog.post('Step '+str(mystep)+' '+step_title[mystep], 'INFO')
    print 'Step ', mystep, step_title[mystep]

# Flagging shadowed data
flagdata(vis = mss,
        mode = 'shadow',
        flagbackup = F)

# Flagging zero value
flagdata(vis = mss,
        mode = 'clip', clipzeros = True, flagbackup = F)

# Flagging edges of channels (TDM)
flagdata(vis = mss,
        spw='0:0~9;116~127,1:0~9;116~127,2:0~9;116~127,3:0~9;116~127',
        mode = 'manual',
        flagbackup = F)

# Flagging of some spws of some antennas (From the result of Tsys cal)
flagdata(vis = mss,
        antenna = 'DV11',
        mode = 'manual',
        flagbackup = F)

flagdata(vis = mss,
        antenna = 'DV25',
        mode = 'manual',
        flagbackup = F)

# Putting a model for the flux calibrator(s)
mystep = 10
if(mystep in thesteps):
    casalog.post('Step '+str(mystep)+' '+step_title[mystep], 'INFO')
    print 'Step ', mystep, step_title[mystep]

#CASA <3>: au.searchFlux('J0522-3627','2015-08-01')
#Source: B0521-365 = J0522-3627 = J0522-364

```

#Requested Freq.: 1-1000 GHz , Requested date: 20150801

# Rank | Flux Density (Jy) | YYYY-MM-DD | Meas. Freq | klambda | Source Name | uvmin-uvmax |

```
# 1 | 5.330 +- .22 | 2015-07-25 | 91.46 GHz | 0.0 | J0522-3627 | 20--657 |
# 2 | 4.570 +- .12 | 2015-07-19 | 343.48 GHz | 0.0 | J0522-3627 | 20--657 |
# 3 | 4.330 +- .6 | 2015-07-19 | 343.48 GHz | 0.0 | J0522-3627 | 20--657 |
# 4 | 5.920 +- .23 | 2015-07-18 | 103.49 GHz | 0.0 | J0522-3627 | 20--657 |
# 5 | 5.740 +- .23 | 2015-07-18 | 91.46 GHz | 0.0 | J0522-3627 | 20--657 |
# 6 | 5.890 +- .3 | 2015-07-05 | 103.49 GHz | 0.0 | J0522-3627 | 20--657 |
# 7 | 5.970 +- .19 | 2015-06-28 | 103.49 GHz | 0.0 | J0522-3627 | 20--657 |
# 8 | 4.370 +- .44 | 2015-06-27 | 343.48 GHz | 0.0 | J0522-3627 | 20--1500 |
# 9 | 6.010 +- .2 | 2015-06-14 | 91.46 GHz | 0.0 | J0522-3627 | 20--657 |
# 10 | 4.760 +- .4 | 2015-06-14 | 337.46 GHz | 0.0 | J0522-3627 | 20--657 |
```

#

#CASA <4>: band3f = 5.920

#CASA <9>: band7f = 4.570

#CASA <6>: band3 = 103.49

#CASA <7>: band7 = 343.48

#CASA <8>: spi = log(band7f/band3f)/log(band7/band3)

#CASA <11>: print spi

# -0.21574826275

```
setjy(vis = mss,
      field = '2', # J0522-3627
      spw = '0,1,2,3',
      standard = 'manual',
      fluxdensity = [5.920, 0, 0, 0],
      spix = -0.215748,
      reffreq = '103.49GHz')
```

# Save flags before bandpass cal

mystep = 11

if(mystep in thesteps):

casalog.post('Step '+str(mystep)+' '+step\_title[mystep], 'INFO')

print 'Step ', mystep, step\_title[mystep]

flagmanager(vis = mss,

mode = 'save',

versionname = 'BeforeBandpassCalibration')

# Bandpass calibration

mystep = 12

if(mystep in thesteps):

casalog.post('Step '+str(mystep)+' '+step\_title[mystep], 'INFO')

print 'Step ', mystep, step\_title[mystep]

os.system('rm -rf'+ mss + '.ap\_pre\_bandpass')

gaincal(vis = mss,

caltable = mss + '.ap\_pre\_bandpass',

field = '1', # J1058+0133

```

scan = '5',
solint = 'int',
refant = 'PM03',
calmode = 'p')

if applyonly != True: es.checkCalTable(mss+'.ap_pre_bandpass', msName=mss,
interactive=False)

os.system('rm -rf '+mss+'.bandpass')
bandpass(vis = mss,
caltable = mss+'.bandpass',
field = '1', # J1058+0133
scan = '5',
solint = 'inf',
refant = 'PM03',
solnorm = True,
bandtype = 'B',
gaintable = mss+'.ap_pre_bandpass')

if applyonly != True: es.checkCalTable(mss+'.bandpass', msName=mss, interactive=False)

# Save flags before gain cal
mystep = 13
if(mystep in thesteps):
casalog.post('Step '+str(mystep)+' '+step_title[mystep], 'INFO')
print 'Step ', mystep, step_title[mystep]

flagmanager(vis = mss,
mode = 'save',
versionname = 'BeforeGainCalibration')

# Gain calibration
mystep = 14
if(mystep in thesteps):
casalog.post('Step '+str(mystep)+' '+step_title[mystep], 'INFO')
print 'Step ', mystep, step_title[mystep]

os.system('rm -rf '+mss+'.phase_int')

gaincal(vis = mss,
caltable = mss + '.phase_int',
field = '1~3', # J1058+0133 J0522-3627 J0854+2006
solint = 'int',
refant = 'PM03',
gaintype = 'G',
calmode = 'p',
gaintable = mss + '.bandpass')

if applyonly != True: es.checkCalTable(mss + '.phase_int', msName=mss, interactive=False)

```

```

os.system('rm -rf'+ mss + '.ampli_inf')
gaincal(vis = mss,
        caltable = mss + '.ampli_inf',
        field = '1~3', # J1058+0133 J0522-3627 J0854+2006
        solint = 'inf',
        refant = 'PM03',
        gaintype = 'T',
        calmode = 'a',
        gaintable = [mss + '.bandpass', mss + '.phase_inf'])

if applyonly != True: es.checkCalTable(mss + '.ampli_inf', msName=mss, interactive=False)

os.system('rm -rf'+mss+'.flux_inf')
os.system('rm -rf'+mss+'.fluxscale')
mylogfile = casalog.logfile()
casalog.setlogfile(mss + '.fluxscale')

fluxscaleDict = fluxscale(vis = mss,
                          caltable = mss + '.ampli_inf',
                          fluxtable = mss + '.flux_inf',
                          reference = '2') # J0522-3627

casalog.setlogfile(mylogfile)

if applyonly != True: es.fluxscale2(caltable = mss+'.ampli_inf', removeOutliers=True,
msName=mss, writeToFile=True, preavg=10000)

os.system('rm -rf'+mss+'.phase_inf')
gaincal(vis = mss,
        caltable = mss+'.phase_inf',
        field = '1~3', # J1058+0133 J0522-3627 J0854+2006
        solint = 'inf',
        refant = 'PM03',
        gaintype = 'G',
        calmode = 'p',
        gaintable = mss+'.bandpass')

if applyonly != True: es.checkCalTable(mss+'.phase_inf', msName=mss, interactive=False)

# Save flags before applycal
mystep = 15
if(mystep in thesteps):
    casalog.post('Step'+str(mystep)+' '+step_title[mystep], 'INFO')
    print 'Step ', mystep, step_title[mystep]

flagmanager(vis = mss,
            mode = 'save',
            versionname = 'BeforeApplycal')

```

```

# Application of the bandpass and gain cal tables
mystep = 16
if(mystep in thesteps):
    casalog.post('Step '+str(mystep)+' '+step_title[mystep],'INFO')
    print 'Step ', mystep, step_title[mystep]

    for i in ['1', '2']: # J1058+0133 J0522-3627
        applycal(vis = mss,
            field = str(i),
            gaintable = [mss + '.bandpass', mss+'.phase_int', mss+'.flux_inf'],
            gainfield = ['', i, i],
            interp = 'linear,linear',
            calwt = T,
            flagbackup = F)

        applycal(vis = mss,
            field = '0,3', # Sun, J0854+2006
            gaintable = [mss+'.bandpass', mss+'.phase_inf', mss+'.flux_inf'],
            gainfield = ['', '3', '3'], # J0854+2006
            interp = 'linear,linear',
            calwt = T,
            flagbackup = F)

# Split out corrected column
mystep = 17
if(mystep in thesteps):
    casalog.post('Step '+str(mystep)+' '+step_title[mystep],'INFO')
    print 'Step ', mystep, step_title[mystep]

    os.system('rm -rf '+mss+'.cal')
    os.system('rm -rf '+mss+'.cal.flagversions')
    split(vis = mss,
        outputvis = mss+'.cal',
        datacolumn = 'corrected',
        timebin='30s',
        keepflags = T)

# Save flags after applycal
mystep = 18
if(mystep in thesteps):
    casalog.post('Step '+str(mystep)+' '+step_title[mystep],'INFO')
    print 'Step ', mystep, step_title[mystep]

    flagmanager(vis = mss+'.cal',
        mode = 'save',
        versionname = 'AfterApplycal')

```

## Appendix C

Following below is the python script used to image and clean solar interferometer data.

```
# JIRA ticket: CSV-3204
# TARGET: Sunspot in NOAA12391 (Epehemris)
# Data ID: uid://A002/Xa72fea/Xd96
# CASA Version for the script: CASA Version 4.4.0

# ALMA Data Reduction Script
# Imaging

#ASDM Directory Name
asdm ='uid__A002_Xa72fea_Xd96'
msc = asdm + '_split.ms.cal'

init = 'F'
cal1_img = 'F'
cal2_img = 'F'
cal3_img = 'F'
sun_img = 'F'

if init == 'T':
    fixplanets(msc, field='0', fixuvw=True, refant='PM03', reftime='median')

#Delete all values in the pointing table
tb.open(msc+'/POINTING', nomodify = False)
a = tb.rownumbers()
tb.removerows(a)
tb.close()

if cal1_img == 'T':
    os.system('rm -rf J1058+0133_all_flux_XX.*')
    clean(vis = msc,
          field='1', #J1058+0133 (Bandpass Calibrator)
          imagename='J1058+0133_all_flux_XX',
          cell = '0.12 arcsec',
          imsize = 1024,
          weighting = 'briggs',
          interactive = T,
          npercycle = 100,
          niter = 1000,
          imagermode='mosaic',
          minpb=0.2,
          stokes='XX',
          pbcor=False)
    os.system('rm -rf J1058+0133_all_flux_YY.*')
    clean(vis = msc,
```

```
field='1', #J1058+0133 (Bandpass Calibrator)
imagename='J1058+0133_all_flux_YY',
cell = '0.12 arcsec',
imsize = 1024,
weighting = 'briggs',
interactive = T,
npercycle = 100,
niter = 1000,
imagermode='mosaic',
stokes='YY',
minpb=0.2,
pbcor=False)
```

```
if cal2_img == 'T':
    os.system('rm -rf J0522-3627_all_flux.*')
    clean(vis = msc,
        field='2', #J0522-3627 (Flux Calibrator)
        imagename='J0522-3627_all_flux',
        cell = '0.12 arcsec',
        imsize = 1024,
        weighting = 'briggs',
        interactive = T,
        npercycle = 100,
        niter = 1000,
        imagermode='mosaic',
        minpb=0.2,
        pbcor=False)
```

```
if cal3_img == 'T':
    os.system('rm -rf J0854+2006_all_flux.*')
    clean(vis = msc,
        field='3', #J0854+2006 (Phase Calibrator)
        imagename='J_all_flux',
        cell = '0.12 arcsec',
        imsize = 1024,
        weighting = 'briggs',
        interactive = T,
        npercycle = 100,
        niter = 1000,
        imagermode='mosaic',
        minpb=0.2,
        pbcor=False)
```

```
if sun_img == 'T':
    #Image synthesis for sun
    os.system('rm -rf A12391_all_ave30s_flux.*')
    #Clean
    clean(vis = msc,
        field='0',
        imagename='A12391_all_ave30s_flux',
        cell = '0.12 arcsec',
```

```
imsize = 2048,  
interactive = T,  
weighting = 'briggs',  
npercycle = 100,  
niter = 20000,  
imagermode='mosaic',  
mask = 0.2,  
minpb = 0.2,  
pbcor=F)
```

Draft



Draft